UNIVERSITY OF CALIFORNIA
RIVERSIDE

Nanoscale Investigations of High Strain Deformation in Magnesium-Yttrium

A Dissertation submitted in partial satisfaction
of the requirements for the degree of

Doctor of Philosophy

in

Materials Science & Engineering

by

Christian John Roach

December 2021

Dissertation Committee:
Dr. Suveen Mathaudhu, Chairperson
Dr. Masaru Rao
Dr. Peter Alexander Greaney

The Dissertation of Christian John Roach is approved:

_____

_____

_____

Committee Chairperson

University of California, Riverside

ACKNOWLEDGEMENTS

I'd like to thank all of those that have helped me along the way. Very briefly; For continued support, in all aspects of my life, my family: Arlette, Christopher, & Brett Roach and Sarah Brashares. For being truly great friends that I could not have made it through grad school without: Trevor Clark, Devin & Ece Coleman, Nicholas Derimow and to each of their families who have been extremely welcoming.

For helping me settle into a new location, continuously inviting me to do things, as well as collect, analyze, and interpret data: Bharat Gwalani. For teaching me useful skills, helping with my research at a new site, and giving useful information and discussions: Liz Kautz, Nicole Overman, Jia Liu, Mark Wirth, Danny Perea, Sten Lambeets, Cheng-Han Li, Arun Bhattacharjee, Julian Escobar, Tingkun Liu, Tanvi Ajatiwalay, Dallin Barton, and Tracy Baker.

For helping me with the science and making it through the lab every day, all my lab mates at UCR: Heather Salvador (especially for helping with some of my Mg work and commiserating over the difficulties with Mg research), Trevor Clark (for helping with research, planning, and de-stressing), Kendrick Mensink, Anqi,'Angel' Yu, Steven Herzberg, Yiwei Sun, Johny Quan, Sina Shahrezaei, Madelyn Madrigal Camacho, Erik Sease, Evander Ramos, Martin Manuel, Josh Edwards, and Adam Feund. For helping me prepare and analyze samples and letting me mentor, my undergrad researchers: Adam Arnot, Lauren Ficarelli, Lauren Oh, Yosuke Inagaki, and Olivia Brandt.

For helping me with sample fabrication, being an employer, mentor, and friend: Roger & the Russell family.

For taking me on and giving me the opportunity to do work at a national lab, teach me new skills, introducing me to useful resources, and helping me grow my professional network: Arun Devaraj

For taking the chance on a non-straight-A student, inviting me in as family, supporting me through difficult times, giving me exceptional opportunities, giving me the hard truths without any ill-will, connecting me to excellent researchers & resources, and helping me to improve: Suveen Mathaudhu.

ABSTRACT OF THE DISSERTATION

Nanoscale Investigations of High Strain Deformation in Magnesium-Yttrium

by

Christian John Roach

Doctor of Philosophy, Graduate Program in Materials Science & Engineering
University of California, Riverside, December 2021
Dr. Suveen Mathaudhu, Chairperson

Refinement to the ultrafine-grain (UFG) regime increases yield strength and improves ductility in magnesium, and high pressure torsion (HPT) enables Mg to be processed to this regime without failure. It is generally agreed that the rate of microstructural refinement scales with applied pressure during HPT, but direct comparisons of pressure's effects during HPT in Mg alloys are scarce.

A dilute Mg-3Y (wt%) alloy was processed to five turns under nominal pressures of 1 GPa, 3 GPa, & 5 GPa. The microstructure was investigated as a function of radius, and thus equivalent strain (ε), by scanning electron microscopy, revealing a shear band-dominated refinement mechanism. Vickers hardness as a function of ε agreed with literature, showing increased refinement rate with pressure, up to a maximum of approximately 90HV at all pressures investigated. TEM was utilized for the nano-scale microstructural investigation at a strain of ε=57 for each pressure, revealing an ultrafine grain structure for the highest pressure and shear bands in the 1 & 3 GPa conditions. APT identifies yttrium segregation to boundaries within the shear band of the 3 GPa ε=57 specimen, and nano-indentation finds that a majority of the hardening comes from within

the core of the shear bands, where the microstructure is in the UFG condition.

Comparison to the broader

The solute segregation as a function of strain was further investigated by APT. In the solutionized condition, no obvious clustering of yttrium is observed and a majority of the solute is in solid solution. At relatively low strain of $\varepsilon=3$, very small clusters of Y are seen segregated at a twin boundary and as the strain is increased to $\varepsilon=16$, the amount of solute segregated and the size of the clusters increases. At a strain of $\varepsilon=57$, the segregation is sizable, with localized solute depletion of the matrix.

Finally, the UFG sizes and solute segregation observed in the Mg3Y are considered in the broader context of the extant literature and the role of solutes is investigated. Solute segregation during deformation stabilizes the fine grains and alters the preferred deformation mechanism, opposing the idea of a true Hall-Petch inversion.

TABLE OF CONTENTS

Contents

List of Figures

List of Tables

Chapter 1 - Introduction

Magnesium production has been steadily increasing for the past several years [1], finding applications in consumer electronics, automotive manufacturing, and other niche structural parts, primarily due to its good strength-to-weight ratio and low density. Magnesium research spiked around WWII, finding applications in military craft as well as consumer goods [2]; unfortunately poor public perception over flammability and corrosion issues, along with increasing capacity and decreasing prices of aluminum, impeded the advancement of magnesium [3]. and it fell out of favor for several decades. Although magnesium is indeed flammable and does not form a native passivation layer, improvements in coating technologies and manufacturing design are increasing the application space for magnesium alloys. The global abundance, recyclability, non-toxicity, and low melting temperature of magnesium make it an attractive option for more eco-friendly metal part production, other pros and cons are listed in Table 1. While magnesium parts can be manufactured by some conventional methods, a large amount of industrial processing still relies on tribal knowledge gained through trial and error, partially due to incomplete fundamental information on the deformation behavior of magnesium alloys under varying and intense strain conditions. Relatively new severe plastic deformation (SPD) processing methods have shown promise in drastically improving the mechanical response of magnesium alloys but in order to fully leverage these, as well as older technologies, a better understanding of the deformation pathways and the role of solutes at an atomic-scale is necessary.

Table 1. Pros and Cons of Magnesium alloys

Pro (+)/Con(-)	Information
+Strength-to-weight	Highest strength-to-weight ratio of structural metals
+Highly recyclable	Recyclability comparable or surpassing Al[4]
+High abundance	7th most abundance in Earth's crust, 0.12 wt% in seawater
+Lowest Production Energy	44kWh/kg, vs 56 kWh/kg for Al and 100 kWh/kg for steel [5]
+Green production	7 CO_2/kg vs 22 CO_2/kg Al and 26 CO_2/kg steel[5]
-Cost of production	Current domestic production cost is $3.31/kg, compared to $2/kg for Al and $0.47/kg for steel[5]
-Flammability	Not suitable for continuous friction environments
-Corrosion	Surface oxide is not coherent and does not passivate, so surface coatings or improved alloys required

In the 1930's Percy W. Bridgman invented an apparatus that allowed the application of shear deformation on solids under high quasi-hydrostatic pressures. The Bridgman 'anvil' (or sometimes 'press') was an exceptional advancement to many scientific disciplines, expanding the limits of achievable pressure and strain. Using his new tool, Bridgman investigated and reported results on over 250 substances within the first few years, eventually leading to his receipt of the 1946 Nobel Prize in Physics. His earliest publications on this technique revealed the ability to imposed very large strains onto many elements, far past their typical yield points, by applying sufficiently high pressures (in the range of 0.1-5 GPa), even in materials which are normally brittle or hard

[6]. His continued research found this to be true in many hexagonal close packed (HCP) metals, which are somewhat notorious for premature failure due to their limited available slip systems [7]. His tool and technique have been adapted and improved, today they are most commonly referred to as High Pressure Torsion (HPT).

Bridgman understood the importance of increasing applied strain, as noted in his first publication on this method [6], though it is doubtful he could have foreseen the exceptional improvements in material properties that result from this process. Some early reports on magnesium alloys revealed submicrometer grains were possible through this technique [8] and recent results show very high ductility in pure magnesium processed by HPT to ultra-fine grain (UFG) sizes [9]. Processing of Mg often results in a textured microstructure and this is also true in HPT, but the intensity of the texture in HPT Mg is lower than other techniques [10]. HPT has also been used to solutionize secondary phases far past equilibrium concentrations into supersaturation [11], even in immiscible Mg-alloys [12].

Arguably the most important factor in HPT is the confinement and quasi-hydrostatic nature of the process; up until the late 90's, the pressure was dependent on back-pressure of the flowing material, but new die designs allow continuous quasi-hydrostatic pressure with limited outward flow [13]. A schematic of an HPT tool and a constrained die design can be seen in figure 1. The minimum pressure required in HPT has been investigated for many materials and the relation has been found to depend predominantly on the shear strength, in order to prevent slippage at the disk-die interface [14]. The importance of hydrostatic pressure has been further informed through back-

pressure equal channel angular pressing (BP-ECAP), an SPD process that can achieve strains similar to HPT[15], [16]. Mg and it's alloys are not typically able to be processed by ECAP, or other SPD techniques at room temperature to sufficiently high strains without premature failure due to the limited available slip systems; however, the application of this confining force allowed Mg & Mg-0.6Y to be processed through 4 passes at ambient temperature and refined to 3μm & 400nm, respectively [17]. Confinement, whether in the case of BP-ECAP or HPT, makes material failure during processing all-but-impossible, allowing very high strains and therefore the homogenization of grain refinement through the entire disk. While it is clear that hydrostatic pressure plays a vital role in these techniques, its impact on the deformation mechanisms has not been thoroughly investigated.

As HPT's usage increased, some investigators did attempt to elucidate pressure's impacts, but many publications are predominantly focused on material properties at saturation, when the refinement rate is balanced with dynamic restoration processes, so the existing pressure studies report this end condition [18]. A few found that the pressure altered the final grain size, but more thorough research concluded that pressure has little effect on the final grain size, provided that the pressure is high enough to prevent slipping [19]–[21]. Some detailed investigations into the evolution of microstructure have been completed, but these are at a single pressure (typically 5-6GPa), and mostly investigate cubic metals; in these systems the microstructural refinement mechanism is found to be fragmentation [22], [23]. The general consensus on pressure is that it affects the rate of refinement, but does not alter the final microstructure in a significant way[24].

Zehetbauer proposed a model as well as measured the vacancy concentration in Ni at various pressures in HPT and reported an increase in the saturation dislocation density and vacancy concentration up to at least 4 GPa, after which he found no further enhancement [21]. He later followed up on this report and inferred that the cause of improved ductility after HPT was that vacancies annihilate dislocations during unloading, causing static recovery [25]. A comparison from Bonarski did find that higher pressure resulted in larger grains in the sample of pure Mg (4 GPa vs 2 GPa), implying that higher pressure may indeed change the final microstructure [10]. This raises the question of whether pressure may alter the microstructural evolution and refinement mechanisms in magnesium alloys.

For the case of cubic systems, fragmentation has been found as the microstructural evolution pathway in several alloys. In HCP systems, there is evidence that other pathways exist; twinning followed by microshear band coalescence has been noted in the case of ECAE [26]. A highly alloyed magnesium processed by HPT at 6 GPa exhibited grain subdivision by multiple twinning and deformation band formation [27]. A similar mechanism to this, twinning dynamic recrystallization (TDRX) was noted by Kaibyshev in some large grained magnesium alloys after more conventional processing techniques [28]. Grain size is known to play a role in the deformation mechanisms in Mg-alloys, with larger grains increasing the propensity for twinning and UFG allowing for grain boundary sliding [29], [30]. Despite multiple reported mechanisms for grain refinement during ambient or low temperature Mg processing, very little has been

presented on what microstructural and processing factors determine the individual microstructural pathways for various alloys and processing methods.

Deformation mechanics can be altered in several ways, most notably here through alloying. Rare-earth (RE) elements are particularly potent in Mg alloys, many of which (including Y) increase the propensity for pyramidal slip over twinning for the accommodation of c-axis deformation [31]. While the magnesium-aluminum-zinc (AZ) system is the most commonly used magnesium alloy, research is still developing on many rare-earth containing systems. Y additions, even at very low concentrations, are able to stabilize UFG grain sizes [32], [33], reduce texturing [34]–[36], and improve strength[37]–[39]. With these benefits, it is worthwhile to further develop our understanding of where yttrium resides in dynamic processing conditions, so that alloys can be engineered with appropriate levels of solutes and processed to the desired microstructures.

Solutes are able to pin boundaries, inhibiting grain growth and dislocation motion, which increases strength and improves microstructural stability. The segregation of solutes to boundaries has been shown to further harden these interfaces and provide unique microstructures which may be leveraged for specific properties [40]. In Mg, the segregation to both tensile and compressive twin boundaries has been extensively documented in Mg-Gd alloys by Nie and others [41]–[44]. Decoration of the twin boundary significantly reduces its mobility and creates a grain boundary drag effect which limits grain growth [45] and reduces texture [46]. Calculations and models for the segregation of solutes to twin boundaries have been created, showing that segregation of

yttrium is favorable [47], [48] and effective at pinning. Strain induced segregation to basal-prismatic interfaces, which may develop into twins, was noted in Mg-1Y after rolling to 2% strain, indicating that this segregation occurs very early in processing [49]. Segregation to grain boundaries has also been observed in several Mg alloys, including Mg-Y, though these usually involve some post-processing thermal treatment [50]–[52]. Strain induced segregation was investigated in Al-Mg processed by HPT at temperatures and concentrations where full solubility was expected; however Mg was seen to segregate to grain boundaries; the mechanism was hypothesized to be diffusion by vacancies, with HPT creating vacancies which move to grain boundaries before annihilating, resulting in a flux of solutes to interfaces [40]. Segregation by strain at room temperature was also observed in a Mg-1Mn-1Nd alloy by HPT and the boundary had saturated in Nd by 1 rotation. This implies that solute segregation in SPD does not follow the expected equilibrium phase diagram and thus must be studied more carefully. It is clear that solutes are able to segregate to boundaries by SPD, but the morphology and concentration may have significant effects on the resulting mechanical properties, thus it is necessary to investigate at an atomic scale.

This leaves several knowledge gaps that need to be addressed in the Mg-Y system processed by HPT:

1. What is the role of pressure in the microstructural evolution and final microstructure of MgY processed by HPT?
2. How does yttrium affect the microstructural evolution of magnesium under SPD conditions?

3. What role does intense shear play on the redistribution of solutes in severely deformed MgY?

Higher pressures clearly cause faster refinement, but these must be reconciled with the higher pressure resulting in larger grains observed by Bonarski [10]. The mechanism for refinement of pure magnesium in HPT has been cited as necklacing [53], but twins and shear bands have been observed in intermediate states for Mg alloys [26], [54]. There have been limited reports of yttrium segregation in Mg [49], [52], [55], but none in the high strain condition at room temperature.

To address the role of pressure, microstructure will be investigated at several levels of strain by scanning electron microscopy (SEM) as well as transmission electron microscopy (TEM) to observe the grain size and structure as processing proceeds. Mechanical properties will be probed by micro- and nano-indentation, to compare the effect of refinement and different microstructural features. To elucidate yttrium's role on the evolution of microstructure in SPD, the progression of refinement obtained by SEM & TEM will be compared to reports in literature of pure magnesium processed under similar conditions, as well as other MgY alloys processed by other techniques. To find the role of shear deformation, atom probe tomography (APT) will be used to identify the location of solutes in the microstructure at an atomic scale, at several levels of strain. This will clarify how segregation develops with increased deformation processing. Lastly, the role of the solutionized Y on the hardness will be explored in the context of the broader role of rare-earth solutes in Mg, with the impacts on the Hall-Petch relationship for different regions of grain sizes and solute contents being addressed.

References

[1] J. J. Barry, G. R. Matos, and W. D. Menzie, "U.S. mineral dependence—Statistical compilation of U.S. and world mineral production, consumption, and trade, 1990–2010:," USGS, U.S. Geological Survey Open-File Report, 2013. [Online]. Available: http://pubs.usgs.gov/of/2013/1184.

[2] C. H. Desch, "Magnesium," *Journal of the Royal Society of Arts*, vol. 91, no. 4638, pp. 272–284, Apr. 1943.

[3] S. N. Mathaudhu and E. A. Nyberg, "MAGNESIUM ALLOYS IN U.S. MILITARY APPLICATIONS: PAST, CURRENT AND FUTURE SOLUTIONS," *Magnesium Technology*, p. 6, 2010.

[4] S. Solar, "Roadmap and test of the Fully Operational MSA for Raw Materialssis," European Commission, Nov. 2015. [Online]. Available: https://ec.europa.eu/jrc/en/scientific-tool/msa

[5] ARPA-E, "METALS Program Overview." DOE, Sep. 2013. [Online]. Available: https://arpa-e.energy.gov/sites/default/files/documents/files/METALS_ProgramSummary.pdf

[6] P. W. Bridgman, "Effects of high shearing stress combined with high hydrostatic pressure," *Physical review*, vol. 48, no. 10, p. 825, Sep. 1935.

[7] P. W. Bridgman, "Shearing Phenomena at High Pressures, Particularly in Inorganic Compounds," *Proceedings of the American Academy of Arts and Sciences*, vol. 71, no. 9, pp. 387–460, 1937.

[8] R. Z. Abdulov, R. Z. Valiev, and N. A. Krasilnikov, "Formation of submicrometre-grained structure in magnesium alloy due to high plastic strains," *Journal of Materials Science Letters*, vol. 9, no. 12, pp. 1445–1447, Dec. 1990, doi: 10.1007/BF00721611.

[9] R. B. Figueiredo, S. Sabbaghianrad, A. Giwa, J. R. Greer, and T. G. Langdon, "Evidence for exceptional low temperature ductility in polycrystalline magnesium processed by severe plastic deformation," *Acta Materialia*, vol. 122, pp. 322–331, Jan. 2017, doi: 10.1016/j.actamat.2016.09.054.

[10] B. J. Bonarski, E. Schafler, B. Mingler, W. Skrotzki, B. Mikulowski, and M. J. Zehetbauer, "Texture evolution of Mg during high-pressure torsion," *Journal of Materials Science*, vol. 43, no. 23–24, pp. 7513–7518, Dec. 2008, doi: 10.1007/s10853-008-2794-8.

[11] W. T. Sun *et al.*, "Exceptional grain refinement in a Mg alloy during high pressure torsion due to rare earth containing nanosized precipitates," *Materials Science and Engineering: A*, vol. 728, pp. 115–123, Jun. 2018, doi: 10.1016/j.msea.2018.05.021.

[12] K. Edalati *et al.*, "Ultra-severe plastic deformation: Evolution of microstructure, phase transformation and hardness in immiscible magnesium-based systems," *Materials Science and Engineering: A*, vol. 701, pp. 158–166, Jul. 2017, doi: 10.1016/j.msea.2017.06.076.

[13] I. V. Alexandrov, Y. T. Zhu, T. C. Lowe, R. K. Islamgaliev, and R. Z. Valiev, "Consolidation of nanometer sized powders using severe plastic torsional straining,"

Nanostructured Materials, vol. 10, no. 1, pp. 45–54, Jan. 1998, doi: 10.1016/S0965-9773(98)00026-9.
[14] D. Kuhlmann-Wilsdorf, B. C. Cai, and R. B. Nelson, "Plastic flow between Bridgman anvils under high pressures," *Journal of Materials Research*, vol. 6, no. 12, pp. 2547–2564, Dec. 1991, doi: 10.1557/JMR.1991.2547.
[15] R. Ye. Lapovok, "The role of back-pressure in equal channel angular extrusion," *Journal of Materials Science*, vol. 40, no. 2, pp. 341–346, Jan. 2005, doi: 10.1007/s10853-005-6088-0.
[16] J. Ribbe *et al.*, "Effect of back pressure during equal-channel angular pressing on deformation-induced porosity in copper," *Scripta Materialia*, vol. 68, no. 12, pp. 925–928, Jun. 2013, doi: 10.1016/j.scriptamat.2013.02.034.
[17] J. Shen, V. Gärtnerová, L. J. Kecskes, K. Kondoh, A. Jäger, and Q. Wei, "Residual stress and its effect on the mechanical properties of Y-doped Mg alloy fabricated via back-pressure assisted equal channel angular pressing (ECAP-BP)," *Materials Science and Engineering: A*, vol. 669, pp. 110–117, Jul. 2016, doi: 10.1016/j.msea.2016.05.067.
[18] A. P. Zhilyaev, G. V. Nurislamova, B.-K. Kim, M. D. Baró, J. A. Szpunar, and T. G. Langdon, "Experimental parameters influencing grain refinement and microstructural evolution during high-pressure torsion," *Acta Materialia*, vol. 51, no. 3, pp. 753–765, Feb. 2003, doi: 10.1016/S1359-6454(02)00466-4.
[19] T. Hebesberger, H. P. Stüwe, A. Vorhauer, F. Wetscher, and R. Pippan, "Structure of Cu deformed by high pressure torsion," *Acta Materialia*, vol. 53, no. 2, pp. 393–402, Jan. 2005, doi: 10.1016/j.actamat.2004.09.043.
[20] F. Wetscher, A. Vorhauer, and R. Pippan, "Strain hardening during high pressure torsion deformation," *Materials Science and Engineering: A*, vol. 410–411, pp. 213–216, Nov. 2005, doi: 10.1016/j.msea.2005.08.027.
[21] M. J. Zehetbauer, J. Kohout, E. Schafler, F. Sachslehner, and A. Dubravina, "Plastic deformation of nickel under high hydrostatic pressure," *Journal of Alloys and Compounds*, vol. 378, no. 1–2, pp. 329–334, Sep. 2004, doi: 10.1016/j.jallcom.2004.01.039.
[22] J. Kratochvil, M. Kruzik, and R. Sedlacek, "A model of ultrafine microstructure evolution in materials deformed by high-pressure torsion," *Acta Materialia*, vol. 57, no. 3, pp. 739–748, Feb. 2009, doi: 10.1016/j.actamat.2008.10.016.
[23] R. Pippan, S. Scheriau, A. Taylor, M. Hafok, A. Hohenwarter, and A. Bachmaier, "Saturation of Fragmentation During Severe Plastic Deformation," *Annu. Rev. Mater. Res.*, vol. 40, no. 1, pp. 319–343, Jun. 2010, doi: 10.1146/annurev-matsci-070909-104445.
[24] A. Zhilyaev and T. Langdon, "Using high-pressure torsion for metal processing: Fundamentals and applications," *Progress in Materials Science*, vol. 53, no. 6, pp. 893–979, Aug. 2008, doi: 10.1016/j.pmatsci.2008.03.002.
[25] M. Zehetbauer, G. Steiner, E. Schafler, A. V. Korznikov, and E. Korznikova, "Deformation Induced Vacancies with Severe Plastic Deformation: Measurements and Modelling," *Materials Science Forum*, vol. 503–504, pp. 57–64, Jan. 2006, doi: 10.4028/www.scientific.net/MSF.503-504.57.

[26] E. Dogan, M. W. Vaughan, S. J. Wang, I. Karaman, and G. Proust, "Role of starting texture and deformation modes on low-temperature shear formability and shear localization of Mg–3Al–1Zn alloy," *Acta Materialia*, vol. 89, pp. 408–422, May 2015, doi: 10.1016/j.actamat.2014.12.006.
[27] L. Tang, Y. Zhao, N. Liang, R. K. Islamgaliev, R. Z. Valiev, and Y. T. Zhu, "Localized deformation via multiple twinning in a Mg–Gd–Y–Zr alloy processed by high-pressure torsion," *Materials Science and Engineering: A*, vol. 677, pp. 68–75, Nov. 2016, doi: 10.1016/j.msea.2016.09.005.
[28] R. Kaibyshev, "Dynamic recrystallization in magnesium alloys," in *Advances in Wrought Magnesium Alloys*, Elsevier, 2012, pp. 186–225. doi: 10.1533/9780857093844.1.186.
[29] M. R. Barnett, "A rationale for the strong dependence of mechanical twinning on grain size," *Scripta Materialia*, vol. 59, no. 7, pp. 696–698, Oct. 2008, doi: 10.1016/j.scriptamat.2008.05.027.
[30] J. Koike, R. Ohyama, T. Kobayashi, M. Suzuki, and K. Maruyama, "Grain-Boundary Sliding in AZ31 Magnesium Alloys at Room Temperature to 523 K," *MATERIALS TRANSACTIONS*, vol. 44, no. 4, pp. 445–451, 2003, doi: 10.2320/matertrans.44.445.
[31] S. Sandlöbes, M. Friák, J. Neugebauer, and D. Raabe, "Basal and non-basal dislocation slip in Mg–Y," *Materials Science and Engineering: A*, vol. 576, pp. 61–68, Aug. 2013, doi: 10.1016/j.msea.2013.03.006.
[32] I. Kawarada, R. Zheng, A. Shibata, H. Somekawa, S. Ogata, and N. Tsuji, "Mechanical Properties and Deformation Mechanism of Mg–Y Alloy with Various Grain Sizes," in *Magnesium Technology 2017*, K. N. Solanki, D. Orlov, A. Singh, and N. R. Neelameggham, Eds. Cham: Springer International Publishing, 2017, pp. 283–287. Accessed: May 02, 2019. [Online]. Available: http://link.springer.com/10.1007/978-3-319-52392-7_41
[33] R. X. Zheng *et al.*, "Effect of Grain Size on Mechanical Properties of Mg-0.3at.%Y Dilute Alloy," *MSF*, vol. 941, pp. 790–795, Dec. 2018, doi: 10.4028/www.scientific.net/MSF.941.790.
[34] T. Al-Samman and X. Li, "Sheet texture modification in magnesium-based alloys by selective rare earth alloying," *Materials Science and Engineering: A*, vol. 528, no. 10–11, pp. 3809–3822, Apr. 2011, doi: 10.1016/j.msea.2011.01.080.
[35] K. Hantzsche, J. Bohlen, J. Wendt, K. U. Kainer, S. B. Yi, and D. Letzig, "Effect of rare earth additions on microstructure and texture development of magnesium alloy sheets," *Scripta Materialia*, vol. 63, no. 7, pp. 725–730, Oct. 2010, doi: 10.1016/j.scriptamat.2009.12.033.
[36] B. Q. Shi, R. S. Chen, and W. Ke, "Effects of yttrium and zinc on the texture, microstructure and tensile properties of hot-rolled magnesium plates," *Materials Science and Engineering: A*, vol. 560, pp. 62–70, Jan. 2013, doi: 10.1016/j.msea.2012.09.010.
[37] A. Akhtar and E. Teghtsoonian, "Solid solution strengthening of magnesium single crystals—I alloying behaviour in basal slip," *Acta Metallurgica*, vol. 17, no. 11, pp. 1339–1349, Nov. 1969, doi: 10.1016/0001-6160(69)90151-5.

[38] A. Kula, X. Jia, R. K. Mishra, and M. Niewczas, "Mechanical Properties of Mg-Gd and Mg-Y Solid Solutions," *Metallurgical and Materials Transactions B*, vol. 47, no. 6, pp. 3333–3342, Dec. 2016, doi: 10.1007/s11663-015-0565-x.
[39] A. Kula, X. Jia, R. K. Mishra, and M. Niewczas, "Flow stress and work hardening of Mg-Y alloys," *International Journal of Plasticity*, vol. 92, pp. 96–121, May 2017, doi: 10.1016/j.ijplas.2017.01.012.
[40] X. Sauvage, A. Duchaussoy, and G. Zaher, "Strain Induced Segregations in Severely Deformed Materials," *MATERIALS TRANSACTIONS*, vol. 60, no. 7, pp. 1151–1158, Jul. 2019, doi: 10.2320/matertrans.MF201919.
[41] M. Bugnet, A. Kula, M. Niewczas, and G. A. Botton, "Segregation and clustering of solutes at grain boundaries in Mg–rare earth solid solutions," *Acta Materialia*, vol. 79, pp. 66–73, Oct. 2014, doi: 10.1016/j.actamat.2014.06.004.
[42] J. P. Hadorn, T. T. Sasaki, T. Nakata, T. Ohkubo, S. Kamado, and K. Hono, "Solute clustering and grain boundary segregation in extruded dilute Mg–Gd alloys," *Scripta Materialia*, vol. 93, pp. 28–31, Dec. 2014, doi: 10.1016/j.scriptamat.2014.08.022.
[43] J. F. Nie, Y. M. Zhu, J. Z. Liu, and X. Y. Fang, "Periodic Segregation of Solute Atoms in Fully Coherent Twin Boundaries," *Science*, vol. 340, no. 6135, pp. 957–960, May 2013, doi: 10.1126/science.1229369.
[44] Y. M. Zhu, M. Z. Bian, and J. F. Nie, "Tilt boundaries and associated solute segregation in a Mg–Gd alloy," *Acta Materialia*, vol. 127, pp. 505–518, Apr. 2017, doi: 10.1016/j.actamat.2016.12.032.
[45] X. Zhao, H. Chen, N. Wilson, Q. Liu, and J.-F. Nie, "Direct observation and impact of co-segregated atoms in magnesium having multiple alloying elements," *Nat Commun*, vol. 10, no. 1, p. 3243, Dec. 2019, doi: 10.1038/s41467-019-10921-7.
[46] C. D. Barrett, A. Imandoust, and H. El Kadiri, "The effect of rare earth element segregation on grain boundary energy and mobility in magnesium and ensuing texture weakening," *Scripta Materialia*, vol. 146, pp. 46–50, Mar. 2018, doi: 10.1016/j.scriptamat.2017.11.004.
[47] Z. Pei, R. Li, J.-F. Nie, and J. R. Morris, "First-principles study of the solute segregation in twin boundaries in Mg and possible descriptors for mechanical properties," *Materials & Design*, vol. 165, p. 107574, Mar. 2019, doi: 10.1016/j.matdes.2018.107574.
[48] J. Zhang, Y. Dou, and Y. Zheng, "Twin-boundary segregation energies and solute-diffusion activation enthalpies in Mg-based binary systems: A first-principles study," *Scripta Materialia*, vol. 80, pp. 17–20, Jun. 2014, doi: 10.1016/j.scriptamat.2014.02.004.
[49] Z. Huang *et al.*, "Dislocation-induced Y segregation at basal-prismatic interfaces in Mg," *Computational Materials Science*, vol. 188, p. 110241, Feb. 2021, doi: 10.1016/j.commatsci.2020.110241.
[50] D. A. Basha, H. Somekawa, and A. Singh, "Crack propagation along grain boundaries and twins in Mg and Mg–0.3 at.%Y alloy during in-situ straining in transmission electron microscope," *Scripta Materialia*, vol. 142, pp. 50–54, Jan. 2018, doi: 10.1016/j.scriptamat.2017.08.023.

[51] J. D. Robson, S. J. Haigh, B. Davis, and D. Griffiths, “Grain Boundary Segregation of Rare-Earth Elements in Magnesium Alloys,” *Metallurgical and Materials Transactions A*, vol. 47, no. 1, pp. 522–530, Jan. 2016, doi: 10.1007/s11661-015-3199-3.
[52] H. Watanabe, A. Owashi, T. Uesugi, Y. Takigawa, and K. Higashi, “Threshold stress for superplasticity in solid solution magnesium alloys,” *Philosophical Magazine*, vol. 92, no. 7, pp. 787–803, Mar. 2012, doi: 10.1080/14786435.2011.634849.
[53] R. B. Figueiredo and T. G. Langdon, “Processing Magnesium and Its Alloys by High-Pressure Torsion: An Overview,” *Adv. Eng. Mater.*, vol. 21, no. 1, p. 1801039, Jan. 2019, doi: 10.1002/adem.201801039.
[54] D. Arpacay, S. B. Yi, M. Janeček, A. Bakkaloglu, and L. Wagner, “Microstructure Evolution during High Pressure Torsion of AZ80 Magnesium Alloy,” *Materials Science Forum*, vol. 584–586, pp. 300–305, Jun. 2008, doi: 10.4028/www.scientific.net/MSF.584-586.300.
[55] X. Wang *et al.*, “Room Temperature Deformation-induced Solute Segregation and its Impact on Twin Boundary Mobility in a Mg-Y Alloy,” *Scripta Materialia*, vol. 209, p. 114375, Mar. 2022, doi: 10.1016/j.scriptamat.2021.114375.

Chapter 2 – Pressure Effects on Microstructural and Hardness Evolution During High Pressure Torsion of Mg Alloys

Christian J. Roach[1,2], Bharat Gwalani[2], Kiran Solanki[3], Arun Devaraj[2*], Suveen Mathaudhu[1,2,4*]

[1]University of California, Riverside, Riverside, CA, USA

[2]Pacific Northwest National Laboratory, Richland, WA, USA

[3]Arizona State University, Tempe, AZ, USA

[4]Colorado School of Mines, Golden, CO, USA

*Co-corresponding authors: smathaudhu@mines.edu and arun.devaraj@pnnl.gov

Abstract

Ultrafine-grained Mg-RE alloys have received recent interested due to their enhanced strength properties, and improved plasticity due to the role of RE's in texture minimization and grain boundary strengthening. Severe plastic deformation (SPD) via high pressure torsion (HPT) has been used to achieve the necessary refinement in grain structure, however review of the extant literature reveals conflicting grain size and hardness outcomes as a function of pressure, and inconsistent mechanisms for the HPT-induced grain refinement. To unravel these reports, microstructure and hardness are probed in a solutionized Mg-3Y wt% (Mg3Y) processed by HPT at pressures of 1 GPa, 3 GPa and 5 GPa. The findings indicated that pressure does not affect the minimum grain size achievable during HPT, however an increased strain (more HPT turns) is required to arrive

at the same grain size (and resultant hardness) when processed with the 1 GPa pressure. The Vickers hardness as a function of applied strain was not representative of the complex microstructures that consisted of various quantities of ultrafine-grained deformation bands, undeformed regions and visible twins, implying the lack of suitability for Vickers hardness as a metric for microstructural saturation. It was observed that ultrafine grains produced by the "SPD within SPD" in the deformation bands generated under any of the tested combinations of applied pressure and strain, resulted in a microstructure that was indicative of the finest grain size and saturated hardness once the Mg3Y was strained enough to produce a homogeneous, uniform ultrafine-grained microstructure. Last, a model was proposed and validated from parallel literature findings that suggest the underlying twin-mediated mechanisms resulting in the generation of the deformation bands, and the textural considerations that would change the deformation mechanism in the same alloy to the commonly-cited necklacing pathway. These collective findings offer insights into processing strategies that may realize ultrafine-grained Mg alloys with enhanced hardness and strength.

Keywords: magnesium, yttrium, severe plastic deformation, nanocrystalline, applied pressure

2.1 Introduction

Grain refinement of magnesium and Mg alloys (hereafter all referred to as "Mg" unless otherwise denoted) to the ultrafine-grained regime (UFG) (100 nm - 1000 nm) via severe plastic deformation (SPD) approaches has been extensively studied in the context of attaining superior superplastic performance [1]–[3]. At ambient temperatures, increases in strength are also generally observed for UFG Mg [4], [5] and more recently some UFG Mg has demonstrated ambient temperature uniform plasticity due to a transition of the dominant deformation mechanisms from twinning and slip to grain boundary rotation and sliding [6], [7]. Exploring thermomechanical processing approaches that arrive at microstructures with the necessary balance of strength and plasticity [8] are therefore of research interest to communities involved in the use of Mg for vehicle and aircraft lightweighting [9], lightweight electronics housings [10] and other applications that may benefit from the potential high-specific strength and energy efficient manufacturability.

A commonly investigated approach for refining microstructures to the UFG or even nanocrystalline (<100 nm) regime is high-pressure torsion (HPT) [11], [12]. Grain refinement is achieved through the imposition of extremely large plastic strains under high quasi-hydrostatic pressure by confinement of the material of interest (Fig. 1). The high-pressure state suppresses failure of the material during the application of strain. More specifically, the combined pressure and shear activates multiple deformation modes, including slip, twinning, and shear banding while simultaneously preventing localizations that lead to failure, even in materials considered to be brittle [13]. This feature is particularly useful for studying grain refinement in Mg, which tends to fail in a brittle

manner at low homologous temperatures due to a limited number of concurrent deformation mechanisms. As with other SPD methods, processing in HPT is usually performed until the microstructural evolution is assumed to be saturated, a steady state condition where further refinement is balanced by dynamic restoration mechanisms [14]. The saturated grain size (d_s) has been referred to as the minimum grain size (d_{min}) [15]; however, as discussed above, d_s depends heavily on processing conditions and thus may be larger than the minimum achievable grain size (d_{min}) [16].

The plastic work during HPT is commonly expressed in terms of shear strain (γ) or equivalent Von Mises strain (ε), which are a function of the number of rotations (N), the distance from the center of rotation (radius (r)), and the post-processing thickness (t), given by Eqns. 1 & 2 [17]:

$$\gamma = \frac{2\pi N \cdot r}{t} \quad \text{Eq. 1}$$

$$\varepsilon = \frac{\gamma}{\sqrt{3}} \quad \text{Eq. 2}$$

Using the assumption that Hall-Petch scaling is valid to ultrafine-grain sizes ($\sigma_y \propto d^{-1/2}$) [18], [19], and that Tabor's analysis holds true ($\sigma_y \propto HV/3$) [20], [21], the vast majority of HPT reports assume that a given material has reached a minimum grain size when the hardness as a function of equivalent strain plateaus. This saturation in hardness is observed to occur at $\varepsilon<20$ for many pure materials when the applied pressure is 6 GPa [14]. In contrast, a recent review by Edalati explored cases of extreme strain $\gamma>1{,}000$ ($\varepsilon>580$) and observed continued changes in hardness and microstructure beyond what was considered

saturation in pure, miscible, and immiscible systems [22]. In addition to microstructural refinement at extreme strains, the role of processing pressure on the microstructural evolution is also minimally reported [23], [24]. At a fundamental level, enough pressure has to be applied to avoid stick-slip interactions with the HPT die that would result in reduced plastic work. The minimum pressure to prevent slipping in the tool is usually taken as three times the flow stress or alternatively, torque measurements may be utilized [25]. Temperature and strain rate are other critical factors which influence microstructural evolution, with lower temperatures or higher strain rates producing a smaller d_s [24]. In elemental or low-alloy systems, purity plays an important role [26]. Even minor solute additions or impurities will increase the stability of grain boundaries and thus decrease the extent of microstructural recovery [27], allowing retention of the induced fine grain sizes.

In an X-ray diffraction study, hydrostatic pressure was shown to decrease the c/a ratio of pure Mg from 1.624 to 1.600 with increasing pressure up to 2.5 GPa, which stays constant with further increases until 7.5 GPa, when it inverts and beings to increase back towards the equilibrium ratio [28]. Combined with the reduction in cell volume, it is expected that hydrostatic pressure may also alter the contributions of Mg's various deformation modes. A viscoplastic self-consistent (VPSC) crystal plasticity model in AZ31 shows a crossover from basal to non-basal dominated slip with increased strain under relatively low hydrostatic pressures of 200 MPa [29]. Indeed, a handful of reports on HPT processed materials have shown variations in hardness and microstructure at the same equivalent strain under different hydrostatic pressures [12]. These reports generally posit that higher pressures produce microstructures equivalent to those from lower pressures, but

in fewer turns, i.e. at a lower equivalent strain, however the mechanisms proposed to explain this phenomena are inconsistent. Some reports have attributed the faster refinement rate to an extension of saturated dislocation density as a function of pressure [30], [31], but others have reported little impact of pressure on saturation microstructures or mechanisms [23], [32], [33].

Overall, the role of pressure is a much less discussed contribution to microstructural evolution during HPT as is its connection to the saturation of grain size. While it is generally agreed that higher pressures result in earlier refinement (i.e. at a lower equivalent strain) and increased homogeneity [12], [14], the few studies that do report the effects of pressure towards refinement are inconsistent in their reported microstructural evolution mechanisms. While some studies have found that elevated pressure results in a higher dislocation density [34], there are other reports of higher pressures resulting in larger grain size, for instance a study on pure Mg processed by HPT found that higher pressure resulted in larger grains at the same strain, in opposition to most observed trends [35]. Some have found higher pressure gave minor reductions in the saturation grain size, which led to small increases in strength [36]–[39] while others have shown saturation microstructures to be pressure invariant so as long as the applied pressure is over a critical value to prevent slipping [23], [40]. Many of these reports probe the behavior of pure metals, where pressure is expected to impact recovery mechanisms, possibly by increased driving force due to increased dislocation or vacancy concentrations [11], [41]–[44]. Solute or alloying additions generally serve to increase the dislocation density during processing and also to

minimize grain boundary mobility, but when compounded with the role of applied pressure, their contributions are largely unexplored.

To better understand and deconvolute the role of pressure on microstructural evolution and hardening during severe plastic deformation, a systematic study varying pressure (1 GPa, 3 GPa, & 5 GPa) and equivalent strain (N<5 turns) on a Mg-3wt%Y alloys has been undertaken, with detailed microstructural and hardness evaluations performed for key processing conditions. The results are then compared to literature reports of microstructural evolution, grain refinement and hardness for multiple pure Mg and Mg alloys processed by HPT, with key trends identified. Our findings suggest that while that increased pressure indeed results in increased grain refinement rate, there is no apparent change in hardness, implying that hardness is a poor predictor of microstructural saturation in Mg and perhaps other materials systems. In Mg and its alloys, the underlying source of this discrepancy lies in evidence for highly diverse microstructural evolution pathways towards grain refinement that are strongly based on microstructural factors affecting starting hardness (e.g. solute concentration, secondary phases, grain size) and the solute electronic effects on deformation mechanisms (e.g. energetics for twinning, stacking faults or slip). These observations forecast the possibility of increasing applied hydrostatic pressure during Mg processing so as to maximize microstructural refinement via different alloy-dependent microstructural evolution pathways.

2.2 Materials and Methods

The binary Magnesium-Yttrium alloy system was selected for this study. While unalloyed magnesium would be of fundamental interest, the low homologous temperatures needed for static or dynamic recrystallization, along with the lack of microstructural contributions that could kinetically suppress grain boundary movement discouraged its use. Solutionized Mg-Y alloys, on the other hand, are reported to undergo preferential solute segregation to grain boundaries given the large atomic radius of Y, and therefore its preference to be in regions with higher free volume, such as grain boundaries [45], [46]. This study by T.J. Lei et al. [45] also reports the segregation of Y partially contributes to the stability of NC grains in ternary Al-alloys. A 25 mm diameter x 50 mm long casting of Mg-3wt%Y (Mg3Y) was acquired from Terves Inc. (Euclid, OH, USA). The rod was sealed in steel foil and homogenized at 550°C for 12 hours in a tube furnace under positive argon atmosphere (0.02 MPa gauge), and was immediately water quenched to maintain the Y in solution. Wire electro-discharge machining (Sodick AQ400L) was used to cut 1.20mm thick slices from which 10 mm disks were punched.

HPT processing was performed on a custom-designed device (fabricated at Ufa State Aviation and Technical University, Ufa, Russia) on 10 mm diameter x 1.20 mm thick disks under quasi-hydrostatic pressure, meaning the sample was upset in the die to a thickness of nominally 1 mm with the flashing from the side providing additional constraints to the pressure (Fig. 1a, flash exaggerated). The samples were processed up 5 rotations under pressures of 1, 3 and 5 GPa at a rotation rate of 1.5 rpm. The 5 GPa pressure

corresponds most closely to the typically applied pressures used for HPT processing (~6 GPa) [12].

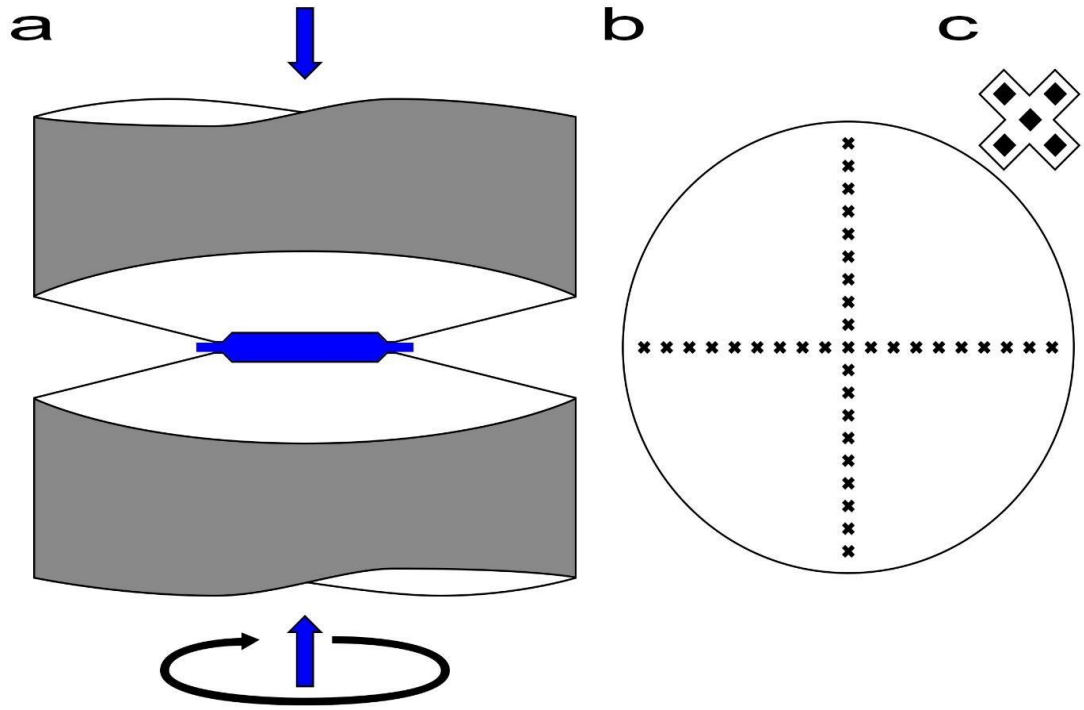

Figure 1. (a) Schematic of quasi-hydrostatic HPT device showing confinement of sample, rotation direction of bottom anvil, and formation of flash from material squeezed out of confinement (not to scale, for illustration only, flash exaggerated). (b) Location of indent groups on surface of a processed sample, incrementally spaced 0.5mm radially, with (c) five individual indents at each "X" marking.

The homogenized and HPT-processed samples were mechanically ground using SiC papers followed by polishing with 1µm alumina on a Chem-Pol polyurethane mat with water-free Red Lube (Allied High Tech, Rancho Dominguez, CA, USA). Final polishing was performed with 0.05 µm water-free colloidal silica on a Final A polyurethane pad (also Allied High Tech) for 1 minute, followed by a brief rinse with deionized water and sonication in ethanol. This procedure was developed to alleviate magnesium alloys' propensity for corrosion and mechanically-induced twinning during polishing.

The average grain size of the annealed slices was determined by visible light microscopy (VLM) using the linear intercept method. Microstructural analysis of the annealed and HPT-processed disks was evaluated on an FEI NovaNano 450 FEG Scanning Electron Microscope (SEM) operating at 5 kV and imaged in backscatter electron (BSE) mode. The refinement as a function of equivalent strain was queried at radii of 1mm and 3.5mm from the center of the disk, which corresponds to equivalent strains of 16 and 57, respectively from Eq. 2. Thin foils were cut on a Helios 660 Focused Ion Beam (FIB)/SEM for each disk at a radius of approximately 3.5mm. Local investigations of microstructure were performed on these foils using a Thermo Fisher Titan Themis 300 Scanning/Transmission Electron Microscope (TEM) operating at 300 kV.

FIB was also used to prepare sharp needles of the annealed and processed (3 GPa at a radius of 3.5 mm from the disk center) material for atomic scale chemical mapping by atom probe tomography (APT). These needles were run in a Cameca LEAP 4000 XHR system at a temperature of 45 K, running in voltage mode with a pulse frequency of 20% at 200kHz with a target evaporation rate of 0.005 atoms/pulse. The data was reconstructed in Integrated Visualization and Analysis Software (IVAS)..

In order to evaluate hardness changes with increased equivalent strain, indentation as a function of radius was performed at 0.5mm increments along the disk diagonals (Fig. 1b) using a Phase II Micro Vickers indenter at 50gf and 15 second creep. Each “x” on Fig. 1b indicates the location of five indents placed nominally as shown on Fig. 1c (not to scale). Indents were performed at distances greater than three indent-diagonal lengths from each other. Nanoindentation was performed in regions with distinct microstructural bands in

order to probe the hardness evolution. A Nanovea mechanical tester (Irvine, CA) with a diamond nano-Berkovich tip was loaded to 200mN per indent at 400mN/min load/unload.

2.3 Results:

The solution annealed material is homogenous, with a large grain size averaging ~1.1mm in diameter (Figure 2a). Fine secondary phase particles are sparse and evenly distributed, as seen in the SEM micrograph (Figure 2b). These particles are yttrium-rich and mostly likely MgY ($Mg_{24}Y_5$) precipitates and yttrium-hydride (YH_2), as has been reported in Mg-rare earth alloys[47]–[49]. APT reconstruction of the annealed material gives a yttrium concentration of 0.56 %at (2.0 %wt) within the annealed needle, with no evidence of segregation. The annealed material is soft, with a Vickers hardness of 41.9±2.0 HV.

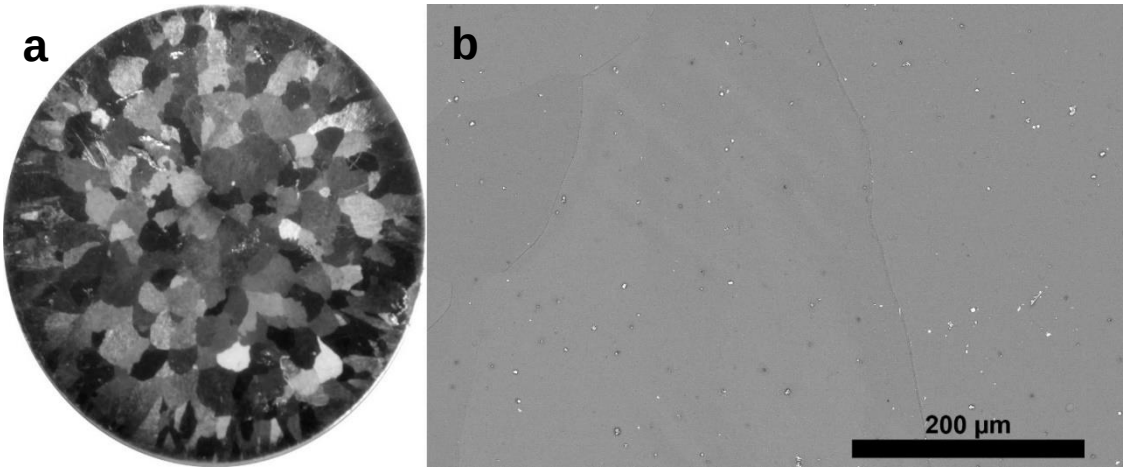

Figure 2. (a) Visible light image of an annealed slice showing large grains, diameter of slice is 24.4 mm. (b) BSE image showing large grain boundaries with scattered secondary phase, scale bar is 200 µm.

Backscattered SEM micrograph images at each processing pressure are presented in Fig. 3 at radii of 1 and 3.5 mm (equivalent strains of 16 and 57, respectively) in samples

processed via five turns. At the lowest pressure of 1 GPa and at ε=16 (Fig. 3a), there is evidence of highly localized deformation along a few narrow bands (white arrows) with some slip traces in the regions between these bands. The region towards the outer edge of the disk with ε=57 (Fig. 3b) consists of a higher density of mostly-parallel deformation bands which are ~2 μm wide and fairly consistently spaced ~20 μm apart. There is limited evidence for twinning seen in the regions between these bands, though some strain accommodation is noted. At a higher pressure of 3 GPa (Fig. 3c), the lower strained region has a microstructure very similar to the higher strained region of the 1 GPa sample, with mostly-parallel, and wider (~6μm) deformation bands, and again are spaced ~20 μm apart. The region between the deformation bands shows more twinning, with several twins aligned in nearly the same direction as the bands. In the larger strained region of the 3 GPa disk (Fig. 3d), the microstructure has a much higher dislocation density, with extensive twinning and deformation bands which cut through one another. The twins also can be observed to bend with the flow of material. The material processed at the highest pressure (5 GPa) shows a microstructure that is mostly UFG but with a few less-refined regions at r=1 (Fig. 3e), while at r=3.5 (Fig. 3f), a homogenous UFG microstructure can be observed.

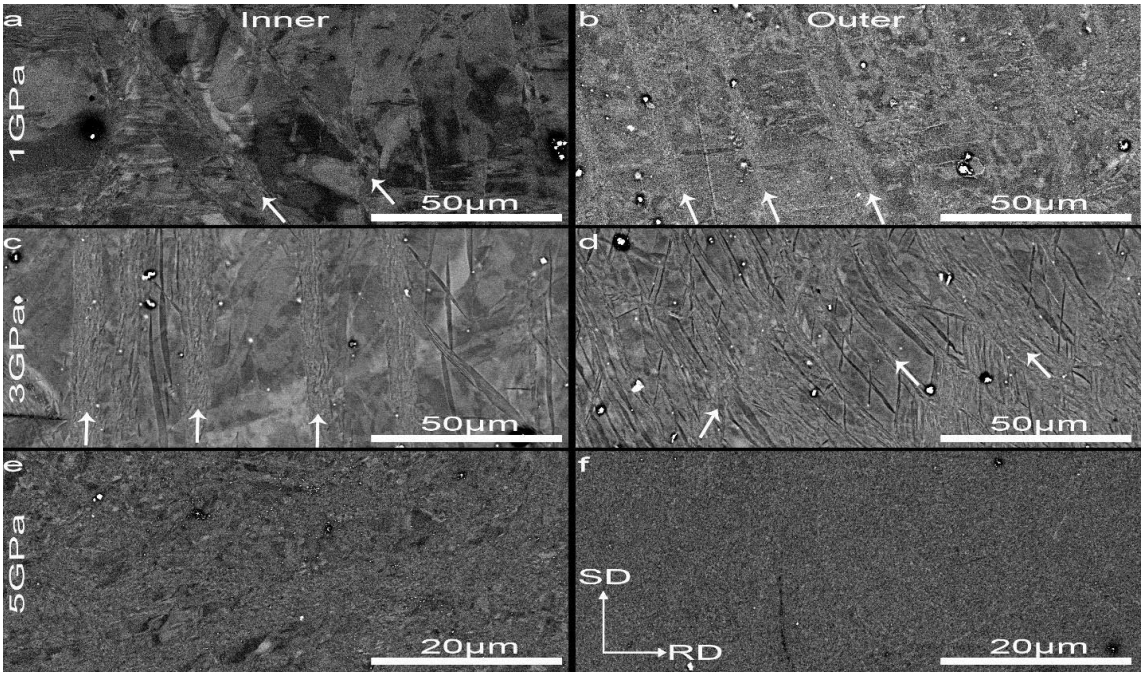

Figure 3. Backscatter SEM images of HPT processed disks. Images taken from the surface in contact with the rotating anvil, at approximate radii of 1mm ("inner" a, c, & e) and 3.5mm ("outer" b, d, & f). White arrows emphasize microstructural bands. The edge of the disk is in the radial direction (RD) to the right, while the direction of force is the shear direction (SD), and is toward the top of the images.

Bright field TEM images from each disk at a radius of 3.5 mm (Fig. 4) provide additional clarity to the microstructures in and outside of the observed bands in Figs. 3b, d and f. At the lowest pressure of 1GPa, a narrow band of elongated grains can be distinguished, with relatively few defects observed outside of this band (Fig. 4a). At the intermediate pressure of 3 GPa, another narrow band of elongated grains with increased defect density is also apparent (Fig. 4b). Either side of the band shows evidence of lattice deformation, however it is expected that the majority of plastic strain in the material in Fig. 4a and 4b is accommodated in the bands rather than the surrounding material. The elongated grains within the bands have widths 100-500nm and lengths that mostly extend over 1 μm. At the highest pressure of 5 GPa, a homogenous UFG microstructure with

grains 100-500nm is seen (Fig. 4c). The defect density within the grains appears to be mixed, with some grains showing residual strain and others with low internal defect densities, consistent with a dynamically recrystallizing microstructure [50] and cellular sub-structures observed in severely deformed Mg alloys [51].

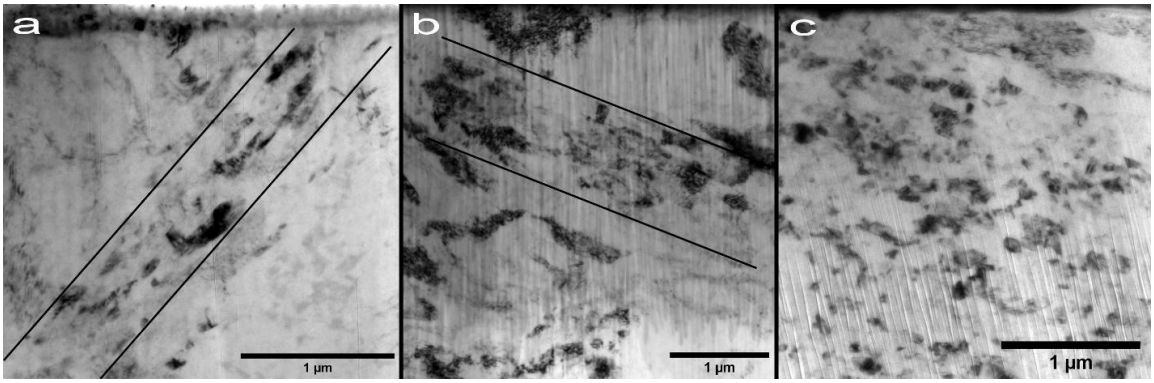

Figure 4. Bright field TEM at a radius of 3.5 mm for 1, 3, and 5 GPa after 5 rotations (a, b, and c respectively). Lines are overlaid to show the strain localization in narrow bands at the lower pressures.

Atom probe tomography was used to further identify the atomic-scale microstructures observed as a function of pressure and strain (Fig. 5). The grain boundaries are decorated with Ga-ions from FIB preparation of the APT sample, and the grain size is again observed to be in the range of 100 nm in the homogenous 5 GPa processed material. No $Mg_{24}Y_5$ precipitates are apparent, and the Y primarily resides along grain boundaries, which likely contributes to retention of the NC grain structures observed [45], [52].

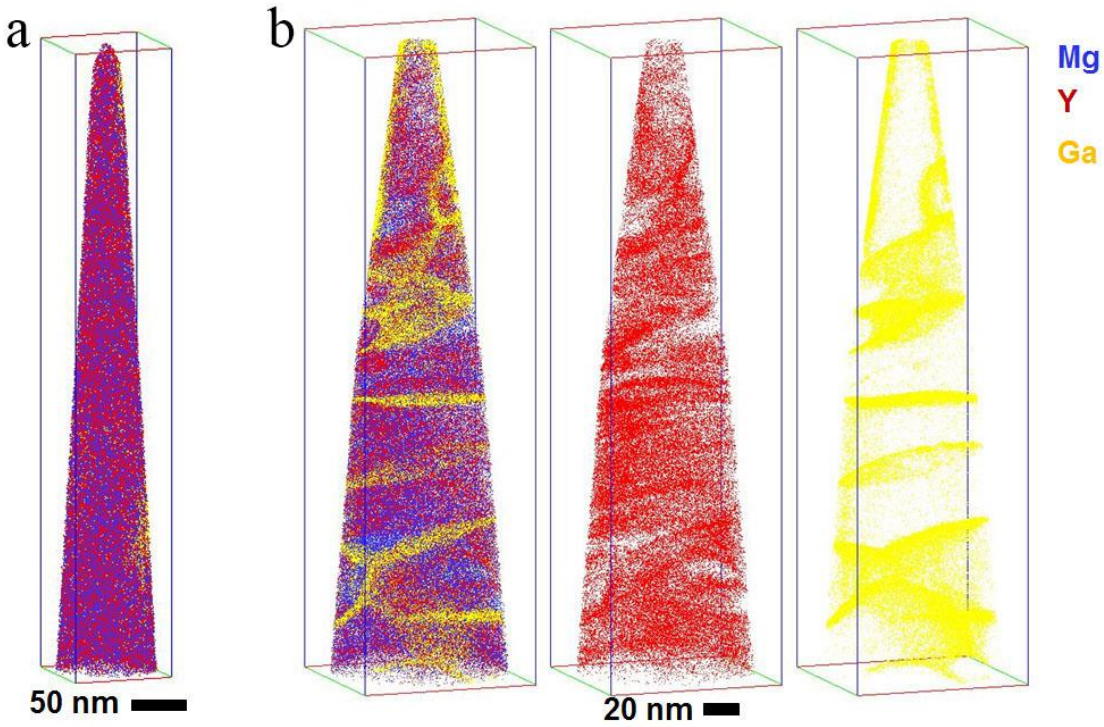

Figure 5. APT reconstructions of the (a) annealed and (b) 3 GPa, 5 turns at radius of 3.5mm. Ga (yellow) decorates grain boundaries.

Vickers microhardness measurements (Fig. 6) at 0.5 mm increments (Fig 1b) show a typical trend of increasing hardness with equivalent strain for all three pressures investigated. Edalati and others [53], [54] have reported that in magnesium alloys processed by HPT, the hardness generally saturates at equivalent strains of ~20. For the 3 GPa and 5 GPa processed materials, the largest increases are seen before ε=20, followed by lesser hardness increases with increasing equivalent strain. The sample processed at 1 GPa shows progressive increases across the full range of equivalent strains tested in this study, reaching a peak hardness of 87±4.6 HV at the outermost radius (r=5). Despite differences in microstructures shown in Fig. 3 and Fig. 4, the hardness values of the 3 and 5 GPa disks are similar across the full range of strains (peak average of 89±4.9 and 87±6.4 HV, respectively). At these Vickers hardness values, the indent diagonals were ~40 μm,

which would result in the interrogation of multiple microstructural features (twins, dislocations, deformation bands) that all contribute in varying proportions to the hardness. To probe the local hardness within individual bands, nanoindentation was implemented and finding individual, narrow bands had very similar hardness to the less refined regions nearby, but locations where bands were large or intersected generally resulted in increased hardness.

2.4 Discussion

The influence of applied pressure during HPT on the microstructure and hardness of magnesium alloys has been reported previously, but studies have largely focused on the steady-state regime. Here, the evolution of microstructure and hardness is investigated at three pressures (1, 3 & 5 GPa). Hardness as a function of equivalent strain follows the trends seen in other literature, with lower pressures requiring larger strains to reach saturation [23], [38]. While there is little difference observed between the 3 & 5 GPa hardness trends, analysis of the SEM reveals clear differences in the underlying microstructures for all pressures investigated (Fig. 3). The APT reconstruction indicates that yttrium is mostly solutionized by the heat treatment, but has segregated to grain boundaries after processing by HPT (Fig. 5), as can be expected under the large deformation conditions provided by HPT [46].

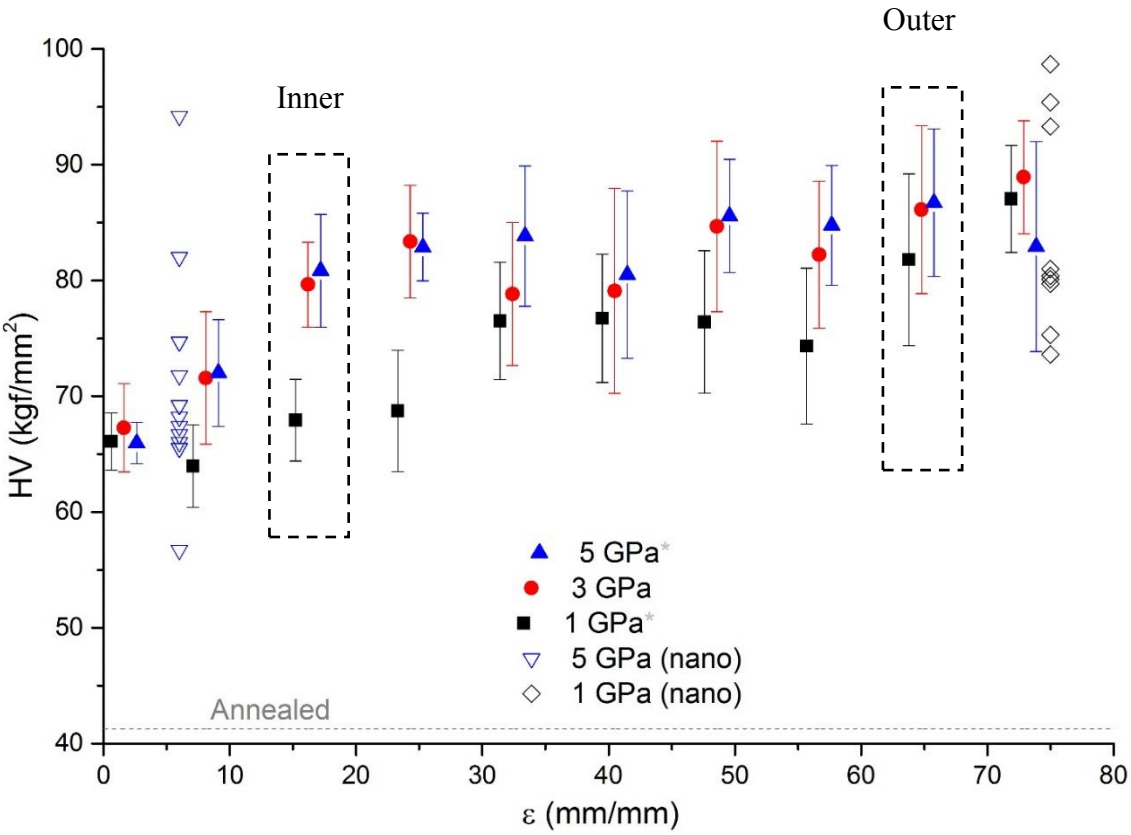

Figure 6. Vickers hardness (HV) vs equivalent strain (ε) for samples processed at each pressure for five HPT turns, as well as an average hardness for the annealed condition. Strain values are offset by -1 and +1 for the disks processed at 1 & 5 GPa, respectively, to improve visual clarity. Range is one standard deviation of 20 data points at each radius. The inverted hollow triangles at ε≈6 and the hollow diamonds at ε≈75 represent nanoindentation measurements made inside and outside the band structures.

Table 1 has data from a survey of the literature for Mg and Mg alloys processed by HPT, and this data is used to generate Fig. 7. This figure presents aggregated data for Vickers Hardness as a function of applied HPT pressure, with the caveat that the reported hardness data represent the average of the maximum saturated hardness at various levels of equivalent strain. Additionally, direct comparisons of the Mg alloys processed at different pressures within the same study are sparse, and only one publication with a direct comparison between pressures was found in Mg for AZ31 [59]. From the materials

explored in this study (Mg3Y), there is no evidence for hardness change as a function of hydrostatic pressure, and the literature generally agrees, showing no clear trends in hardness with pressure for equivalent alloys or nearly equivalent alloys. These results are consistent with reports of Edalati and Horita [23]. There is also an implicit assumption that the hardness saturates independent of pressure based on the formation of equivalent microstructures, albeit at higher ε for lower pressures. [23], [37] The higher values of hardness of the literature-reported Mg alloys in Fig. 7 compared to the Mg3Y in this study are in-part related to the total amount of solute present in the individual alloy. As reported by Edalati & Horita, the hardness at saturation shows a strong trend with solute concentration [23]. Most solutes in Mg increase hardness, but as reported elsewhere, Li softens Mg, even after very high strains. [22], [64]

The observations of Edalati and Horita and Hebesberger et al. that hardness saturation is independent of pressure is ascribed to the eventual arrival at similar microstructural features after enough strain, with the conventional microstructural feature being the smallest average grain size. [23], [38] The microstructures observed in our Mg3Y alloy as a function of pressure and applied strain call this observation into question, given the large variety of microstructural features present that exhibit equivalent hardness. For example, the data in the "outer" range for 3 GPa and 5 GPa on Fig. 6 show hardness values that are very similar, however inspection of the microstructures from these regions (3GPa/Fig. 3d and 5GPa/Fig. 3f), reveals very different microstructures. The material processed under 3 GPa pressure shows periodic deformation banding while at the same equivalent strain under 5 GPa the sample is

marked by a uniform microstructure with fine grains. Therefore, the source of the equivalent hardness from different microstructures necessitates more exploration.

Table 2. Literature and experimental data for HPT processed pure Mg and Mg alloys

Alloy (wt%)	**P [GPa]**	**N**	**C [wt%]**	**d_{avg} [nm]**	**HV [kgfmm^2]**	**Ref**
AZ31	1	20	4.5		100	[55]
AZ31	2.5	15	4.5	150-250	115	[56]
AZ31	6	20	4.5	200	120	[55]
AZ80	3	15	9.3		125	[57]
AZ80	6	10	9.3	200	120	[58]
AZ91	3	5	10.0		125	[59]
AZ91	6	10	10.0		135	[59]
ZK60	2	5	6.2	700±500	120	[60]
ZK60	6	7	6.2		123	[55]
Mg3Y	1	5	3.0		89	This work
Mg3Y	3	5	3.0		89	This work
Mg3Y	5	5	3.0		89	This work
Mg8Li	3	5	8.0	500	63	[61]
Mg8Li	6	5	8.0		45	[22]
Mg-10.6Zn-3.3Y	2.5	10	13.0	150	130	[62]
Mg-8.1Zn-5.1Y	5	7	13.2	53	120	[63]

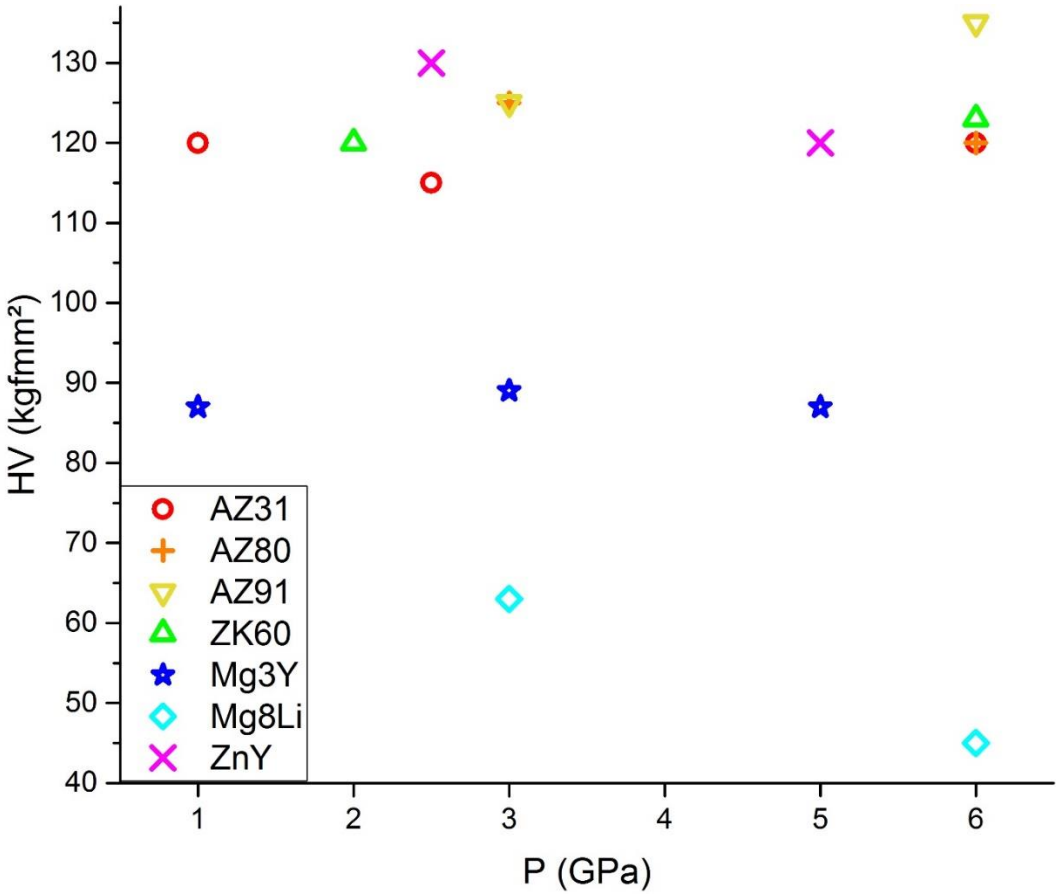

Figure 7. Plot of Vickers hardness (HV) vs applied pressure for Mg alloys cited in Table.

Overall, the evolution of the Mg3Y microstructures appear to be driven by deformation band formation and evolution, as seen in Figures 3 & 4, and consistent with microstructural evolution models proposed by Dogan et al. [65]–[67] Figure 3a shows relatively few, narrow bands, and closer inspection indicates that they are likely twins. Twinning is a common deformation mechanism in Mg alloys, with the main twin type being tensile $\{10\bar{1}2\}$ twins. Contraction $\{10\bar{1}1\}$ twins are much less operative but the associated lattice reorientation often leads to preferential slip & secondary twinning within the twinned volume, which causes strain softening and often leads to failure by void coalescence [68]. While this mechanism can lead to failure under ambient conditions, in

the confined conditions of HPT, it is reasonable to predict that a contraction twin would become a preferential site for strain localization. Nanoindentation measurements were performed inside and outside the deformation bands as shown, along with approximate indentation locations (green triangles) in Fig. 8. Fig. 8a presents a sample processed under a low pressure condition (1 GPa), but at the outer edge of the disk in a region of high strains ($\varepsilon \approx 75$). Material in the shear bands is measured to be harder (~93 kgf/mm^2) as compared to the material between the deformation bands (~87 kgf/mm^2). Per the trends from Fig. 6, these accurately represent the average hardness expect for this amount of equivalent strain. Similarly, Fig. 8b give the same measurements for material processed under a higher pressure (5 GPa), but near the center of the disk where the strain is quite low ($\varepsilon \approx 6$). In this case, areas of intersecting narrow shear bands demonstrate hardness values of >68 kgf/mm^2 while the regions free of bands show lower hardness values (<67 kgf/mm^2). Comparison with Fig. 6 again reveals typical hardness values for this equivalent strain at P=5 GPa, $\varepsilon \approx 6$. In both samples shown in Fig. 8, the highest hardness observed is within the shear bands or at the intersection of shear bands, and the hardness in these regions is consistent with the maximum average hardness values at saturation (~87 kgf/mm^2) as shown in Fig. 7. This finding suggests that even at low pressures and low strains, the ultrafine (100–500 nm) grains observed in the deformation bands (Fig. 4) determine the maximum hardness achievable at saturation. In a sense, the shear bands that form during HPT of the Mg3Y represent "SPD within SPD" with the progressive generation and interactions of the bands tending towards microstructural homogeneity, as demonstrated by uniform UFG structures, with increasing equivalent strain during processing. Returning to the

observations of equivalent hardness for vastly different microstructures; this may be accounted for by the size of Vickers microhardness indentations compared to the size of microstructural features. The distance between deformation bands is seen to be on the order of 25μm in Figs. 3b & 3c, and this distance decreases with increasing pressure and/or equivalent strain. The diagonal of the Vickers indentations is greater than 30 μm for all cases, indicating the possibility of the indenter probing regions containing both the heavily refined shear bands and the minimally deformed inter-band regions at the same time, and thereby giving an "average" value for hardness.

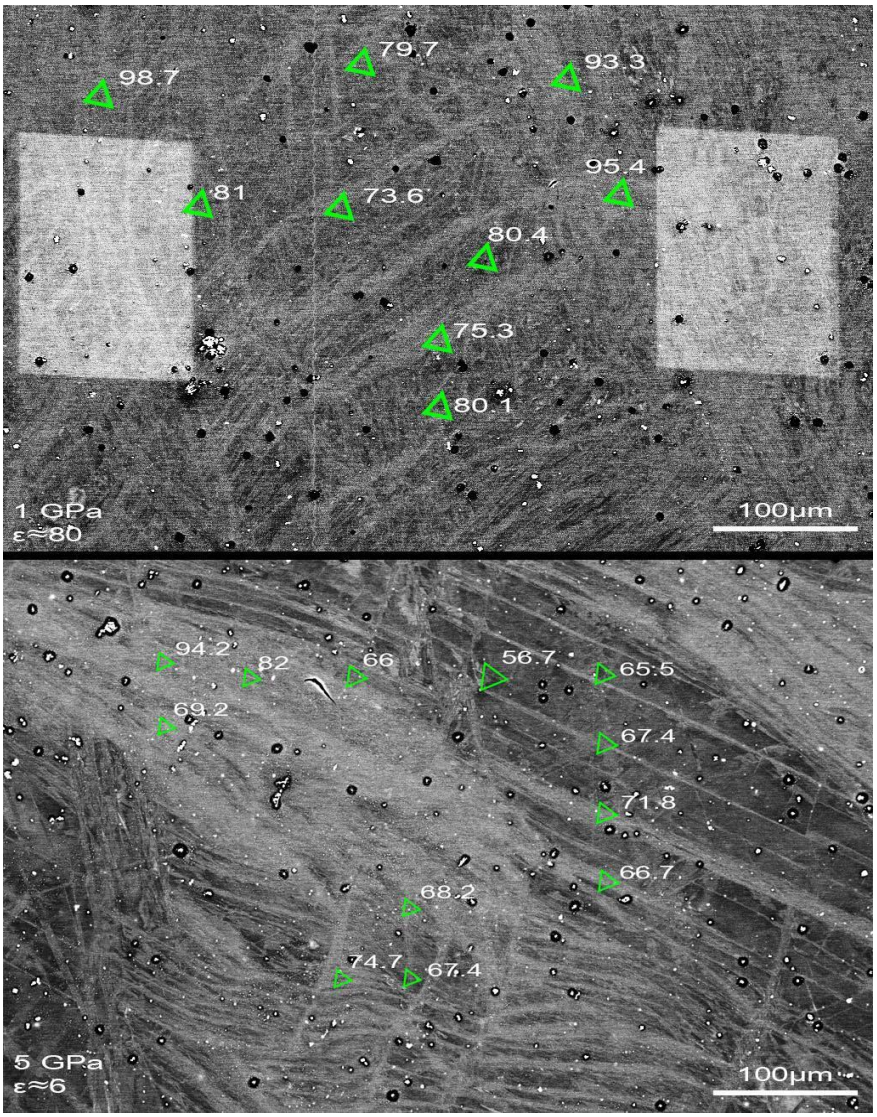

Figure 8. Backscatter SEM images of microstructures observed in Mg3Y HPT processed at: a) 1 GPa and ε=75, and b) 5 GPa and ε=6. The overlaid green triangles give the locations of the nanoindentation measurements within and outside of the bands.

Literature-reported assumptions of microstructural contributions to hardness, as typically defined by grain size, stem from a commonly reported model for microstructural refinement in Mg alloys. Namely, the suggested microstructural evolution pathway in HPT at room temperature is speculated to be the same as elevated temperature SPD methods, such as equal channel angular pressing (ECAP) [69]. Under these assumptions, the primary

microstructural refinement during ambient HPT of Mg and its alloys is claimed to be necklacing (progressive dynamic recrystallization of fine grains in the highly-sheared intergranular regions) [69]. Other literature however, reports strain localization and banding without necklacing, especially at lower pressures, to play a predominant role in refinement [56], [57], [59], [70]. The work by Kang et al. [71] in part, alludes to the root of such contradictory observations by showing that hydrostatic pressure achieved through backpressure during ECAP alters the predominant deformation mechanisms in an AZ31 alloy [71] by increasing the <c+a> activity and reducing the common necklacing effect. Through the application of back-pressure, Fatemi-Varzaneh et al. observed microstructural refinement along wide shear bands during accumulative back extrusion, but did not provide a mechanism for the band formation. [72], [73]

A clear mechanistic pathway to the microstructural evolution via intersecting deformation bands was put forward by Tang et al., who performed room temperature HPT on a solutionized Mg-8Gd-3Y-0.4Zr (wt%) alloy with processing conditions (6.0 GPa, ambient temperature and 1 rpm up to five rotations) very similar to those used for the Mg3Y studied here (5.0 GPa, ambient temperature and 1.5 rpm up to five turns). [67] Subdivision of the starting grains by a variety of twin boundaries was observed, along with the formation of recrystallized grains within deformation bands and the concurrent presence of narrow twins. They proposed that grain refinement occurs via the sequential activation of localized multiple twinning and the formation of deformation bands. [67]

To tie collective findings on the role of pressure and microstructural evolution together, a model for microstructural evolution in Mg-alloys when the conditions or alloys

favor microstructural refinement by increased intersectional deformation banding [56], [59], [66] is proposed (Fig. 9).

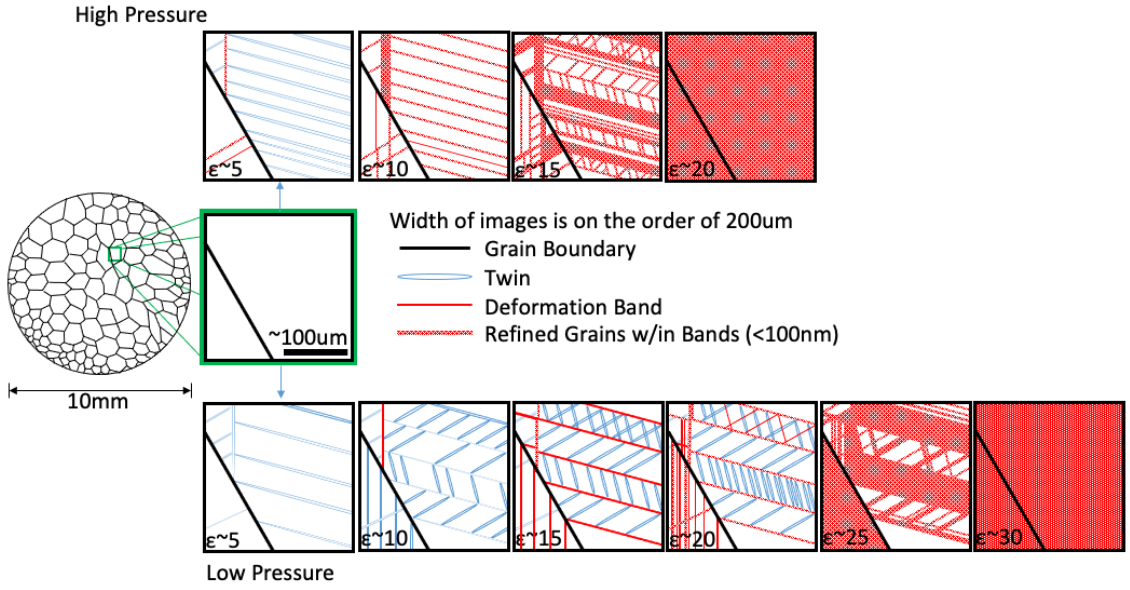

Figure 9. Model schematic for grain refinement during low or high pressures HPT processing.

Figure 9 depicts the following sequence of events for low pressure HPT processing. At low equivalent strains (ε≈5), twins form in preferential orientation and broaden, as evidenced by slip traces in wide twins, and some grains, assumed to be in the "hard" orientation, do not contain twins. With increasing equivalent strain, previous twins convert to deformation bands (~5 mm wide, ε≈10), followed by the generation and intersection of more deformation bands (ε≈15). Then at higher strains (ε>30), deformation bands have broadened and the microstructure is dominated by intersecting twins or deformation bands (>10 mm wide). At high pressures, a similar progression of refinement occurs, but with less equivalent strain. At low strains (ε≈5) the microstructure consists of a few narrow deformation bands and many more parallel twins than observed for the same strain in the

low pressure case. At ε≈10 the deformation bands have broadened to ~10 mm wide, with evidence for intersecting shear bands with intersecting twins between them. With increasing strain (ε≈15), broad regions of ultrafine grains have formed with evidence of some thin and thick deformation bands remaining. Lastly, at ε>20 the microstructure is nearly fully composed of ultrafine grains.

This model is consistent with the "multiple twinning" model suggested by Tang et al. [67] and a model proposed by Dogan et al., [66] for specific starting texture (basal poles initially parallel to the extrusion direction) in a Mg AZ31 alloy ECAP processed at 150°C. They posit that grain refinement occurs via compression twins and double twins causing localized deformation wherein dynamic recrystallization occurred. Plastic flow concentrates in the deformation bands due to localized high basal slip activity within the bands, which leads to repetitive dynamic recrystallization and more intersecting micro-shear bands. In their study, these dynamically recrystallized regions initiated a macro shear band resulting in sample failure, however given the high confinement pressures associated with HPT, and their role in suppressing fracture, no such failure was observed in this study. Again, this is consistent with the study by Kang et al. [71] that the imposition of back-pressure (i.e. a strong confining pressure) suppresses the formation of tension twins that eventually weaken and cause macro-localization, however this is not the full explanation. Dogan et al. [66] used the equivalent ECAP processing for the same Mg AZ31 alloy, but with the basal poles initially perpendicular to the extrusion direction, and this sample did not fail via macro shear localization. Microstructural analysis of this sample revealed the conventional necklace features comprised of fine dynamically recrystallized grains

accumulated in grain boundaries. These findings point to the starting material texture having a heavy influence on observed microstructural refinement during severe plastic deformation. With the basal poles oriented parallel to the extrusion direction, tensile double twins and compressive twins, followed by basal slip in the reoriented twin regions inform the microstructural evolution and grain refinement. When the basal poles are oriented perpendicular to the extrusion direction, prismatic slip is the predominant deformation mode which resulted in continuous dynamic recrystallization and necklacing. While texture was not measured in this study, it can now be speculated that the basal poles were oriented parallel to the shear direction imposed during HPT.

Another consideration that may have contributed to the deformation of the Mg3Y alloy during HPT stems from the observed role of Y in weakening texture which resulted in enhanced room temperature plasticity, [74] which was also suggested by Tang et al. for the HPT processed Mg-8Gd-3Y-0.4Zr (wt%) alloy. [67] These reports assume the uniform distribution of the Y solute in the lattice, however recent work has shown that room temperature deformation alone is enough to relocate Y solutes along coherent twin boundaries, and suppress twin boundary mobility. [46] This is consistent with the location of solute observed in the APT reconstruction shown in Fig. 6. Given the potential for RE solutes to modify the interfacial energy characteristics [75]and therefore the deformation mechanisms in Mg-RE alloys, further investigation on the implications of HPT-driving RE solute segregations to the nanocrystalline grain boundaries is warranted.

2.5 Conclusion

A Mg-3wt%Y alloy was HPT processed at three different pressures to study the role of pressure on hardening and microstructural refinement, and to resolve a number of conflicting reports on the role of pressure and on the mechanisms for grain refinement in Mg-alloys. The study arrived at the following findings:

1) Varying the applied pressure from 1 GPa to 5 GPa did not result in any differences in the maximum hardness after HPT processing. The pressure was observed to influence the amount of applied strain needed to achieve the maximum hardness state, with the necessary total strain needed for maximum hardness increasing with decreasing applied pressure. These findings are consistent with those reported for multiple materials by Edalati and Horita and on pure Cu by Hebesberger et al. [23], [38], suggesting that this correlation is pervasive across materials that do not undergo phase transformation during processing. Reports of grain growth during increased pressure HPT processing can be reconciled by the likelihood of dynamic recrystallization and grain growth in the pure Mg that was studied[35].
2) While Vickers hardening for the Mg3Y alloys processed at 3 GPa and 5 GPa followed the same trends, microstructural analysis revealed different underlying microstructures in both states. The microstructures are composed of ultrafine-grained deformation bands of varying thickness and density as a function of applied strain. The similarity of trends is attributed to the Vickers indenter interrogating broad regions composed of deformation banded and unbanded regions. This finding

also suggests that Vickers microhardness be carefully implemented if the intention is to infer microstructural saturation and homogeneity from saturated hardness, as local microstructural heterogeneities may not be revealed.

3) Nanoindentation studies correlated with TEM of the deformation bands at various pressures indicate that the ultrafine grains (100–500 nm) formed in deformation bands in the early stages of HPT processing, whether at low or high pressures, are predictive of the smallest uniform average grain size (~ 200 nm) achievable and the maximum hardness achievable (~85 kgf/mm^2) after increased applied strain. With the addition of strain, the "SPD within SPD" continues via the formation of more intersecting shear bands that eventually arrive at homogenous ultrafine-grained state.

4) Contrary to the commonly reported necklacing mechanism for grain refinement during severe plastic deformation [69], the Mg3Y in this study refines through the activity of multiple intersecting twin-nucleated deformation bands. A model is proposed for how this process proceeds under low- and high- pressure confinement. This model is consistent with the microstructural evolution observed in an HPT-processed Mg-RE alloy [67] and a low temperature ECAP processed Mg AZ31 alloy with the texture oriented such that the basal plane lie parallel to the extrusion directions [66]. In both studies, dynamic recrystallization initiated due to heavy basal slip activity in the reoriented lattice within compression twins and double-twins. In the Dogan et al study, changing the textural orientation so that the basal planes are perpendicular to the extrusion direction results in deformation mediated

by prismatic slip, resulting in refinement via the necklacing mechanism. [66] This finding indicated the importance of the initial crystallographic texture on the microstructural evolution mechanisms and grain refinement in Mg alloys and perhaps other metals with non-cubic, anisotropic crystal structures.

Declaration of Competing Interest

The authors declare that they have no known competing financial interests or personal relationships that could have appeared to influence the work reported in this paper.

Acknowledgements

CJR, KS and SNM were supported in part via the US National Science Foundation grant #1463679.

CJR was hosted at the US Department of Energy's (DOE) Pacific Northwest National Laboratory via support from a DOE Office of Science Graduate Student Research (SCGSR) Program Fellowship. AD would like to acknowledge the laboratory directed research and development (LDRD) funding as a part of Solid Phase Processing Science Initiative (SPPSi) from Pacific Northwest National Laboratory

References

[1] M. Kai, Z. Horita, and T. G. Langdon, "Developing grain refinement and superplasticity in a magnesium alloy processed by high-pressure torsion," *Materials Science and Engineering: A*, vol. 488, no. 1–2, pp. 117–124, Aug. 2008, doi: 10.1016/j.msea.2007.12.046.

[2] R. Panicker, A. H. Chokshi, R. K. Mishra, R. Verma, and P. E. Krajewski, "Microstructural evolution and grain boundary sliding in a superplastic magnesium AZ31 alloy," *Acta Materialia*, vol. 57, no. 13, pp. 3683–3693, Aug. 2009, doi: 10.1016/j.actamat.2009.04.011.

[3] H. Watanabe, T. Mukai, M. Mabuchi, and K. Higashi, "Superplastic deformation mechanism in powder metallurgy magnesium alloys and composites," *Acta Materialia*, vol. 49, no. 11, pp. 2027–2037, Jun. 2001, doi: 10.1016/S1359-6454(01)00101-X.

[4] M. Al-Maharbi *et al.*, "Microstructure, crystallographic texture, and plastic anisotropy evolution in an Mg alloy during equal channel angular extrusion processing," *Materials Science and Engineering: A*, vol. 528, no. 25–26, pp. 7616–7627, Sep. 2011, doi: 10.1016/j.msea.2011.06.043.

[5] D. C. Foley, M. Al-Maharbi, K. T. Hartwig, I. Karaman, L. J. Kecskes, and S. N. Mathaudhu, "Grain refinement vs. crystallographic texture: Mechanical anisotropy in a magnesium alloy," *Scripta Materialia*, vol. 64, no. 2, pp. 193–196, Jan. 2011, doi: 10.1016/j.scriptamat.2010.09.042.

[6] R. B. Figueiredo, S. Sabbaghianrad, A. Giwa, J. R. Greer, and T. G. Langdon, "Evidence for exceptional low temperature ductility in polycrystalline magnesium processed by severe plastic deformation," *Acta Materialia*, vol. 122, pp. 322–331, Jan. 2017, doi: 10.1016/j.actamat.2016.09.054.

[7] Z. Zeng, J.-F. Nie, S.-W. Xu, C. H. J. Davies, and N. Birbilis, "Super-formable pure magnesium at room temperature," *Nature Communications*, vol. 8, no. 1, Dec. 2017, doi: 10.1038/s41467-017-01330-9.

[8] K. Wei *et al.*, "Grain size effect on tensile properties and slip systems of pure magnesium," *Acta Materialia*, vol. 206, p. 116604, Mar. 2021, doi: 10.1016/j.actamat.2020.116604.

[9] S. N. Mathaudhu and E. A. Nyberg, "MAGNESIUM ALLOYS IN U.S. MILITARY APPLICATIONS: PAST, CURRENT AND FUTURE SOLUTIONS," *Magnesium Technology*, p. 6, 2010.

[10] S. R. Agnew, J. W. Senn, and J. A. Horton, "Mg sheet metal forming: Lessons learned from deep drawing Li and Y solid-solution alloys," *JOM*, vol. 58, no. 5, pp. 62–69, May 2006, doi: 10.1007/s11837-006-0026-8.

[11] K. Edalati and Z. Horita, "A review on high-pressure torsion (HPT) from 1935 to 1988," *Materials Science and Engineering: A*, vol. 652, pp. 325–352, Jan. 2016, doi: 10.1016/j.msea.2015.11.074.

[12] A. Zhilyaev and T. Langdon, "Using high-pressure torsion for metal processing: Fundamentals and applications," *Progress in Materials Science*, vol. 53, no. 6, pp. 893–979, Aug. 2008, doi: 10.1016/j.pmatsci.2008.03.002.

[13] B. Zheng *et al.*, “Multiple and extended shear band formation in MgCuGd metallic glass during high-pressure torsion,” *Scripta Materialia*, vol. 86, pp. 24–27, Sep. 2014, doi: 10.1016/j.scriptamat.2014.04.023.
[14] R. Pippan, S. Scheriau, A. Taylor, M. Hafok, A. Hohenwarter, and A. Bachmaier, “Saturation of Fragmentation During Severe Plastic Deformation,” *Annu. Rev. Mater. Res.*, vol. 40, no. 1, pp. 319–343, Jun. 2010, doi: 10.1146/annurev-matsci-070909-104445.
[15] F. A. Mohamed and S. S. Dheda, “On the minimum grain size obtainable by high-pressure torsion,” *Materials Science and Engineering: A*, vol. 558, pp. 59–63, Dec. 2012, doi: 10.1016/j.msea.2012.07.066.
[16] B. Yang, H. Vehoff, A. Hohenwarter, M. Hafok, and R. Pippan, “Strain effects on the coarsening and softening of electrodeposited nanocrystalline Ni subjected to high pressure torsion,” *Scripta Materialia*, vol. 58, no. 9, pp. 790–793, May 2008, doi: 10.1016/j.scriptamat.2007.12.039.
[17] R. Z. Valiev, Yu. V. Ivanisenko, E. F. Rauch, and B. Baudelet, “Structure and deformaton behaviour of Armco iron subjected to severe plastic deformation,” *Acta Materialia*, vol. 44, no. 12, pp. 4705–4712, Dec. 1996, doi: 10.1016/S1359-6454(96)00156-5.
[18] E. O. Hall, *Yield Point Phenomena in Metals and Alloys*. Boston, MA: Springer US, 1970. doi: 10.1007/978-1-4684-1860-6.
[19] P. Zhang, S. X. Li, and Z. F. Zhang, “General relationship between strength and hardness,” *Materials Science and Engineering: A*, vol. 529, pp. 62–73, Nov. 2011, doi: 10.1016/j.msea.2011.08.061.
[20] J. R. Cahoon, W. H. Broughton, and A. R. Kutzak, “The determination of yield strength from hardness measurements,” *Metallurgical Transactions*, vol. 2, no. 7, pp. 1979–1983, Jul. 1971.
[21] D. Tabor, “The hardness and strength of metals,” *JOURNAL OF THE INSTITUTE OF METALS*, vol. 79, pp. 1–18, 1951.
[22] K. Edalati, “Metallurgical Alchemy by Ultra-Severe Plastic Deformation via High-Pressure Torsion Process,” *MATERIALS TRANSACTIONS*, vol. 60, no. 7, pp. 1221–1229, Jul. 2019, doi: 10.2320/matertrans.MF201914.
[23] K. Edalati and Z. Horita, “Universal Plot for Hardness Variation in Pure Metals Processed by High-Pressure Torsion,” *MATERIALS TRANSACTIONS*, vol. 51, no. 5, pp. 1051–1054, 2010, doi: 10.2320/matertrans.M2009431.
[24] R. Pippan, F. Wetscher, M. Hafok, A. Vorhauer, and I. Sabirov, “The Limits of Refinement by Severe Plastic Deformation,” *Advanced Engineering Materials*, vol. 8, no. 11, pp. 1046–1056, Nov. 2006, doi: 10.1002/adem.200600133.
[25] R. E. Riecker, L. C. Towle, and T. P. Rooney, “SHEAR STRENGTH OF TWELVE GROSSLY DEFORMED METALS AT HIGH PRESSURES AND TEMPERATURES\,” p. 35, Aug. 1967.
[26] K. Edalati *et al.*, “Influence of dislocation–solute atom interactions and stacking fault energy on grain size of single-phase alloys after severe plastic deformation using high-pressure torsion,” *Acta Materialia*, vol. 69, pp. 68–77, May 2014, doi: 10.1016/j.actamat.2014.01.036.

[27] Y. Ito, K. Edalati, and Z. Horita, “High-pressure torsion of aluminum with ultrahigh purity (99.9999%) and occurrence of inverse Hall-Petch relationship,” *Materials Science and Engineering: A*, vol. 679, pp. 428–434, Jan. 2017, doi: 10.1016/j.msea.2016.10.066.
[28] G. L. Clendenen and H. G. Drickamer, “Effect of Pressure on the Volume and Lattice Parameters of Magnesium,” *Physical Review*, vol. 135, no. 6A, pp. A1643–A1645, Sep. 1964, doi: 10.1103/PhysRev.135.A1643.
[29] H. Wang, P. D. Wu, S. Y. Lee, J. Wang, and K. W. Neale, “Numerical study of the effects of shear deformation and superimposed hydrostatic pressure on the formability of AZ31B sheet at room temperature,” *International Journal of Mechanical Sciences*, vol. 92, pp. 70–79, Mar. 2015, doi: 10.1016/j.ijmecsci.2014.12.002.
[30] M. Zehetbauer, G. Steiner, E. Schafler, A. V. Korznikov, and E. Korznikova, “Deformation Induced Vacancies with Severe Plastic Deformation: Measurements and Modelling,” *Materials Science Forum*, vol. 503–504, pp. 57–64, Jan. 2006, doi: 10.4028/www.scientific.net/MSF.503-504.57.
[31] M. J. Zehetbauer, J. Kohout, E. Schafler, F. Sachslehner, and A. Dubravina, “Plastic deformation of nickel under high hydrostatic pressure,” *Journal of Alloys and Compounds*, vol. 378, no. 1–2, pp. 329–334, Sep. 2004, doi: 10.1016/j.jallcom.2004.01.039.
[32] K. Edalati, E. Matsubara, and Z. Horita, “Processing Pure Ti by High-Pressure Torsion in Wide Ranges of Pressures and Strain,” *Metall and Mat Trans A*, vol. 40, no. 9, pp. 2079–2086, Sep. 2009, doi: 10.1007/s11661-009-9890-5.
[33] M. Kawasaki, B. Ahn, and T. G. Langdon, “Microstructural evolution in a two-phase alloy processed by high-pressure torsion,” *Acta Materialia*, vol. 58, no. 3, pp. 919–930, Feb. 2010, doi: 10.1016/j.actamat.2009.10.007.
[34] M. J. Zehetbauer, H. P. Stüwe, A. Vorhauer, E. Schafler, and J. Kohout, “The Role of Hydrostatic Pressure in Severe Plastic Deformation,” *Advanced Engineering Materials*, vol. 5, no. 5, pp. 330–337, May 2003, doi: 10.1002/adem.200310090.
[35] B. J. Bonarski, E. Schafler, B. Mingler, W. Skrotzki, B. Mikulowski, and M. J. Zehetbauer, “Texture evolution of Mg during high-pressure torsion,” *Journal of Materials Science*, vol. 43, no. 23–24, pp. 7513–7518, Dec. 2008, doi: 10.1007/s10853-008-2794-8.
[36] M. Hafok and R. Pippan, “Influence of stacking fault energy and alloying on stage V hardening of HPT-deformed materials,” *International Journal of Materials Research*, vol. 101, no. 9, pp. 1097–1104, Sep. 2010, doi: 10.3139/146.110389.
[37] T. Hebesberger, H. P. Stüwe, A. Vorhauer, F. Wetscher, and R. Pippan, “Structure of Cu deformed by high pressure torsion,” *Acta Materialia*, vol. 53, no. 2, pp. 393–402, Jan. 2005, doi: 10.1016/j.actamat.2004.09.043.
[38] T. Hebesberger, R. Pippan, and H. P. Stüwe, “Effect of Pressure on the Final Grain Size after High Pressure Torsion,” in *Ultrafine Grained Materials II*, Y. T. Zhu, T. G. Langdon, R. S. Mishra, S. L. Setniatin, M. J. Saran, and T. C. Lowe, Eds. Hoboken, NJ, USA: John Wiley & Sons, Inc., 2013, pp. 133–140. doi: 10.1002/9781118804537.ch16.

[39] F. Wetscher, A. Vorhauer, and R. Pippan, “Strain hardening during high pressure torsion deformation,” *Materials Science and Engineering: A*, vol. 410–411, pp. 213–216, Nov. 2005, doi: 10.1016/j.msea.2005.08.027.
[40] A. Hohenwarter, A. Bachmaier, B. Gludovatz, S. Scheriau, and R. Pippan, “Technical parameters affecting grain refinement by high pressure torsion,” *International Journal of Materials Research*, vol. 100, no. 12, pp. 1653–1661, Dec. 2009, doi: 10.3139/146.110224.
[41] T. I. Chashchukhina, M. V. Degtyarev, and L. M. Voronova, “Effect of pressure on the evolution of copper microstructure upon large plastic deformation,” *The Physics of Metals and Metallography*, vol. 109, no. 2, pp. 201–209, Feb. 2010, doi: 10.1134/S0031918X10020122.
[42] K. Edalati, Y. Hashiguchi, H. Iwaoka, H. Matsunaga, R. Z. Valiev, and Z. Horita, “Long-time stability of metals after severe plastic deformation: Softening and hardening by self-annealing versus thermal stability,” *Materials Science and Engineering: A*, vol. 729, pp. 340–348, Jun. 2018, doi: 10.1016/j.msea.2018.05.079.
[43] B. Oberdorfer *et al.*, “Absolute concentration of free volume-type defects in ultrafine-grained Fe prepared by high-pressure torsion,” *Scripta Materialia*, vol. 63, no. 4, pp. 452–455, Aug. 2010, doi: 10.1016/j.scriptamat.2010.05.007.
[44] E. Schafler, “Effect of Hydrostatic Pressure on the Microstructure and Mechanical Properties during and after High Pressure Torsion,” *Materials Science Forum*, vol. 667–669, pp. 657–664, Dec. 2010, doi: 10.4028/www.scientific.net/MSF.667-669.657.
[45] T. Lei, J. Shin, D. S. Gianola, and T. J. Rupert, “Bulk nanocrystalline Al alloys with hierarchical reinforcement structures via grain boundary segregation and complexion formation,” *Acta Materialia*, vol. 221, p. 117394, Dec. 2021, doi: 10.1016/j.actamat.2021.117394.
[46] X. Wang *et al.*, “Room Temperature Deformation-induced Solute Segregation and its Impact on Twin Boundary Mobility in a Mg-Y Alloy,” *Scripta Materialia*, vol. 209, p. 114375, Mar. 2022, doi: 10.1016/j.scriptamat.2021.114375.
[47] Y. Huang, L. Yang, S. You, W. Gan, K. U. Kainer, and N. Hort, “Unexpected formation of hydrides in heavy rare earth containing magnesium alloys,” *Journal of Magnesium and Alloys*, vol. 4, no. 3, pp. 173–180, Sep. 2016, doi: 10.1016/j.jma.2016.08.002.
[48] M. Janecek *et al.*, “Mechanical properties and microstructure of magnesium alloy Mg22Gd processed by severe plastic deformation,” *Advanced Materials Letters*, vol. 8, no. 9, pp. 897–904, Jun. 2017, doi: 10.5185/amlett.2017.1582.
[49] S. M. Zhu, J. F. Nie, M. A. Gibson, and M. A. Easton, “On the unexpected formation of rare earth hydrides in magnesium–rare earth casting alloys,” *Scripta Materialia*, vol. 77, pp. 21–24, Apr. 2014, doi: 10.1016/j.scriptamat.2014.01.007.
[50] R. Kaibyshev, “Dynamic recrystallization in magnesium alloys,” in *Advances in Wrought Magnesium Alloys*, Elsevier, 2012, pp. 186–225. doi: 10.1533/9780857093844.1.186.

[51] B. Li, E. Ma, and K. T. Ramesh, “Dislocation Configurations in an Extruded ZK60 Magnesium Alloy,” *Metall and Mat Trans A*, vol. 39, no. 11, pp. 2607–2614, Nov. 2008, doi: 10.1007/s11661-008-9621-3.
[52] Z. Huang *et al.*, “Dislocation-induced Y segregation at basal-prismatic interfaces in Mg,” *Computational Materials Science*, vol. 188, p. 110241, Feb. 2021, doi: 10.1016/j.commatsci.2020.110241.
[53] K. Edalati, A. Yamamoto, Z. Horita, and T. Ishihara, “High-pressure torsion of pure magnesium: Evolution of mechanical properties, microstructures and hydrogen storage capacity with equivalent strain,” *Scripta Materialia*, vol. 64, no. 9, pp. 880–883, May 2011, doi: 10.1016/j.scriptamat.2011.01.023.
[54] C. L. P. Silva, I. C. Tristão, S. Sabbaghianrad, S. A. Torbati-Sarraf, R. B. Figueiredo, and T. G. Langdon, “Microstructure and Hardness Evolution in Magnesium Processed by HPT,” *Materials Research*, vol. 20, no. suppl 1, pp. 2–7, Sep. 2017, doi: 10.1590/1980-5373-mr-2017-0223.
[55] L. R. C. Malheiros, R. B. Figueiredo, and T. G. Langdon, “Processing Different Magnesium Alloys through HPT,” *Materials Science Forum*, vol. 783–786, pp. 2617–2622, May 2014, doi: 10.4028/www.scientific.net/MSF.783-786.2617.
[56] J. Stráská, M. Janeček, J. Gubicza, T. Krajňák, E. Y. Yoon, and H. S. Kim, “Evolution of microstructure and hardness in AZ31 alloy processed by high pressure torsion,” *Materials Science and Engineering: A*, vol. 625, pp. 98–106, Feb. 2015, doi: 10.1016/j.msea.2014.12.005.
[57] D. Arpacay, S. B. Yi, M. Janeček, A. Bakkaloglu, and L. Wagner, “Microstructure Evolution during High Pressure Torsion of AZ80 Magnesium Alloy,” *Materials Science Forum*, vol. 584–586, pp. 300–305, Jun. 2008, doi: 10.4028/www.scientific.net/MSF.584-586.300.
[58] S. A. Alsubaie, P. Bazarnik, M. Lewandowska, Y. Huang, and T. G. Langdon, “Evolution of microstructure and hardness in an AZ80 magnesium alloy processed by high-pressure torsion,” *Journal of Materials Research and Technology*, vol. 5, no. 2, pp. 152–158, Apr. 2016, doi: 10.1016/j.jmrt.2015.11.006.
[59] A. Al-Zubaydi, R. B. Figueiredo, Y. Huang, and T. G. Langdon, “Structural and hardness inhomogeneities in Mg–Al–Zn alloys processed by high-pressure torsion,” *Journal of Materials Science*, vol. 48, no. 13, pp. 4661–4670, Jul. 2013, doi: 10.1007/s10853-013-7176-1.
[60] S. A. Torbati-Sarraf, S. Sabbaghianrad, R. B. Figueiredo, and T. G. Langdon, “Orientation imaging microscopy and microhardness in a ZK60 magnesium alloy processed by high-pressure torsion,” *Journal of Alloys and Compounds*, vol. 712, pp. 185–193, Jul. 2017, doi: 10.1016/j.jallcom.2017.04.054.
[61] H. Matsunoshita, K. Edalati, M. Furui, and Z. Horita, “Ultrafine-grained magnesium–lithium alloy processed by high-pressure torsion: Low-temperature superplasticity and potential for hydroforming,” *Materials Science and Engineering: A*, vol. 640, pp. 443–448, Jul. 2015, doi: 10.1016/j.msea.2015.05.103.
[62] P. Jenei, J. Gubicza, E. Y. Yoon, and H. S. Kim, “X-ray diffraction study on the microstructure of a Mg–Zn–Y alloy consolidated by high-pressure torsion,” *Journal*

of Alloys and Compounds, vol. 539, pp. 32–35, Oct. 2012, doi: 10.1016/j.jallcom.2012.05.100.
[63] Y. Li, J. Wang, and R. Xu, "The microstructure and mechanical properties of nanocrystalline Mg-Zn-Y alloy achieved by a combination of aging and high pressure torsion," *Vacuum*, vol. 178, p. 109396, Aug. 2020, doi: 10.1016/j.vacuum.2020.109396.
[64] T. Al-Samman, "Comparative study of the deformation behavior of hexagonal magnesium–lithium alloys and a conventional magnesium AZ31 alloy," *Acta Materialia*, vol. 57, no. 7, pp. 2229–2242, Apr. 2009, doi: 10.1016/j.actamat.2009.01.031.
[65] Y. Cao, S. Ni, X. Liao, M. Song, and Y. Zhu, "Structural evolutions of metallic materials processed by severe plastic deformation," *Materials Science and Engineering: R: Reports*, vol. 133, pp. 1–59, Nov. 2018, doi: 10.1016/j.mser.2018.06.001.
[66] E. Dogan, M. W. Vaughan, S. J. Wang, I. Karaman, and G. Proust, "Role of starting texture and deformation modes on low-temperature shear formability and shear localization of Mg–3Al–1Zn alloy," *Acta Materialia*, vol. 89, pp. 408–422, May 2015, doi: 10.1016/j.actamat.2014.12.006.
[67] L. Tang, Y. Zhao, N. Liang, R. K. Islamgaliev, R. Z. Valiev, and Y. T. Zhu, "Localized deformation via multiple twinning in a Mg–Gd–Y–Zr alloy processed by high-pressure torsion," *Materials Science and Engineering: A*, vol. 677, pp. 68–75, Nov. 2016, doi: 10.1016/j.msea.2016.09.005.
[68] M. R. Barnett, "Twinning and the ductility of magnesium alloys Part II. 'Contraction' twins," *Materials Science and Engineering: A*, vol. 464, no. 1–2, pp. 8–16, Aug. 2007, doi: 10.1016/j.msea.2007.02.109.
[69] R. B. Figueiredo and T. G. Langdon, "Processing Magnesium and Its Alloys by High-Pressure Torsion: An Overview," *Adv. Eng. Mater.*, vol. 21, no. 1, p. 1801039, Jan. 2019, doi: 10.1002/adem.201801039.
[70] S. Panda *et al.*, "Analysis of heterogeneities in strain and microstructure in aluminum alloy and magnesium processed by high-pressure torsion," *Materials Characterization*, vol. 123, pp. 159–165, Jan. 2017, doi: 10.1016/j.matchar.2016.11.027.
[71] F. Kang, J. Q. Liu, J. T. Wang, and X. Zhao, "The effect of hydrostatic pressure on the activation of non-basal slip in a magnesium alloy," *Scripta Materialia*, vol. 61, no. 8, pp. 844–847, Oct. 2009, doi: 10.1016/j.scriptamat.2009.07.011.
[72] S. M. Fatemi-Varzaneh, A. Zarei-Hanzaki, and S. Izadi, "Shear deformation and grain refinement during accumulative back extrusion of AZ31 magnesium alloy," *J Mater Sci*, vol. 46, no. 6, pp. 1937–1944, Mar. 2011, doi: 10.1007/s10853-010-5029-8.
[73] S. M. Fatemi-Varzaneh and A. Zarei-Hanzaki, "Processing of AZ31 magnesium alloy by a new noble severe plastic deformation method," *Materials Science and Engineering: A*, vol. 528, no. 3, pp. 1334–1339, Jan. 2011, doi: 10.1016/j.msea.2010.10.033.

[74] B. Q. Shi, R. S. Chen, and W. Ke, “Effects of yttrium and zinc on the texture, microstructure and tensile properties of hot-rolled magnesium plates,” *Materials Science and Engineering: A*, vol. 560, pp. 62–70, Jan. 2013, doi: 10.1016/j.msea.2012.09.010.
[75] H. Zhou *et al.*, “Effect of Ag on interfacial segregation in Mg–Gd–Y–(Ag)–Zr alloy,” *Acta Materialia*, vol. 95, pp. 20–29, Aug. 2015, doi: 10.1016/j.actamat.2015.05.020.

Chapter 3 – Grain Boundary Solute Segregation During Ambient Temperature High Pressure Torsion Processing of a Mg-Y Alloy

Christian Roach[a,b], Cheng-Han Li[b], Bharat Gwalani[b], Arun Devaraj[b*], Suveen Mathaudhu[a,b,c*]

[a]University of California, Riverside, CA, USA

[b]Physical and Computational Sciences Directorate, Pacific Northwest National Laboratory, Richland, WA, USA

[c]Colorado School of Mines, Golden, CO, USA

*Co-corresponding authors: smathaudhu@mines.edu and arun.devaraj@pnnl.gov,

Abstract

The presence of rare earth solutes on boundaries in magnesium has been correlated with improved strength and texture reduction. Solute segregation is typically driven by a thermal treatment after straining a solutionized alloy. High pressure torsion can impart very high strains, resulting in the generation of complex defect structures which alter segregation kinetics. In this work, segregation of yttrium to boundaries after ambient temperature high pressure torsion is demonstrated, pointing to deformation-driven pathways to grain boundary engineering in Mg-RE alloys.

Keywords: Magnesium; yttrium; solute segregation; high pressure torsion; solute clustering;

3.1 Introduction

The segregation of rare earth (RE) solutes to twin and grain boundaries in magnesium has been correlated with improved strength and reduced texture, while enabling smaller stable grain sizes [1]. Models have shown that yttrium is potent for these beneficial effects, prefers boundary sites, and engenders thermal stability against grain growth [2], making it a good candidate for alloying. Reports of solute segregation by strain in magnesium often involve post-processing thermal treatments. Annealing alone can drive solute segregation by diffusion [3], but strain processing imparts additional energy and defect pathways to increase segregation [4]. More recently, Mg-3Y (wt%) alloy compressed to 2% strain has shown completely deformation-driven solute segregation to dislocation cores, twin boundaries, and basal facets [5]. High pressure torsion (HPT) is able impart very high strains into a material, forming complex defect structures which may provide alternative fast-diffusion pathways, leading to interfaces rich in solute. While segregation by large strain at room temperature has been reported in a few materials [6], large strain conditions have not been investigated for Mg-Y alloys. Here we report the segregation of yttrium in a dilute magnesium alloy at room temperature by HPT through a range of equivalent strains (ε=3, 16, and 57). These findings forecast the microstructural engineering of dilute Mg-RE alloys for targeted mechanical properties.

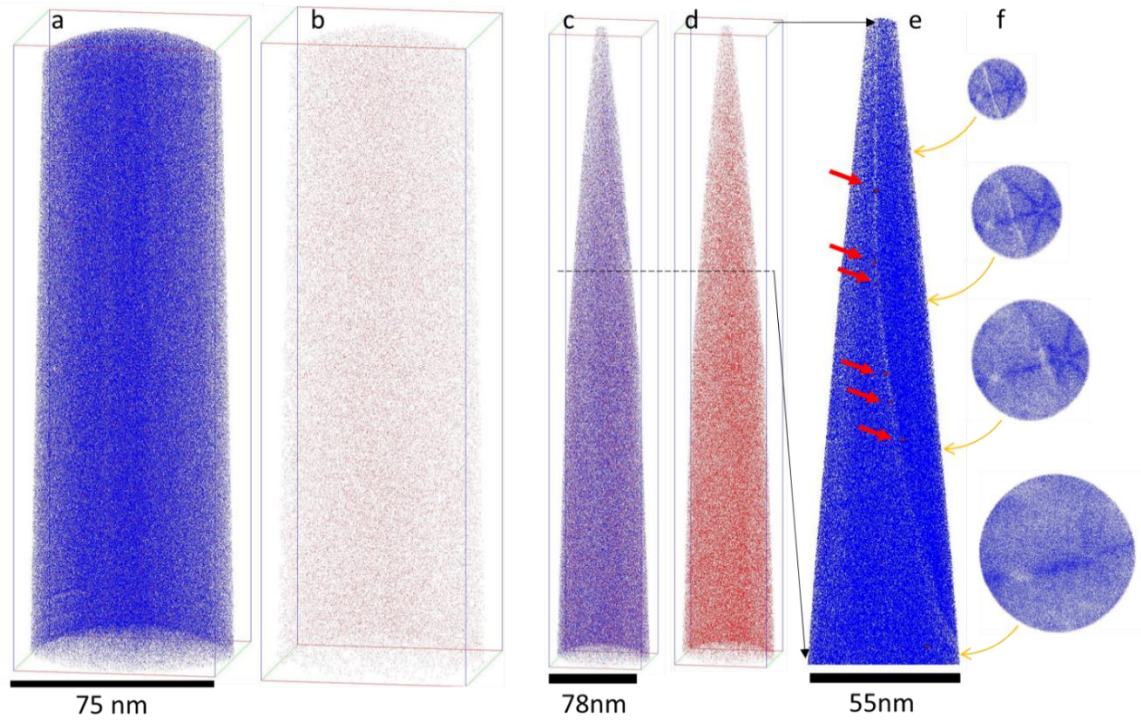

Figure 10. Atom probe tomography reconstructions of (a & b) the annealed Mg3Y and (c, d, e, & f) the Mg3Y at ε=3. The annealed sample shows (a) all ions with no obvious features and (b) homogenously distributed Y containing species throughout the sample. The ε=3 sample shows a boundary with all ions displayed (c) but the Y species alone do not show obvious clustering. Zooming in to a 25nm thick slice of the top 255nm of the needle shows the boundary clearly in Mg ions (e) with the 3 at% Y isosurface revealing small clusters within the boundary. The pole figures (f) from 10nm thick slices in the Z axis, indicating the boundary is likely a twin.

3.2 Materials & Methods

As-cast binary Mg3Y alloy (Terves Inc Euclid, OH, USA) was solutionized at 550°C for 12 hours in an argon cover-gas furnace, and quenched in water. This material was cut into thin sheets (1.2mm thick) from which ø10mm disks were punched. These disks were processed by HPT at nominal pressures of 5 GPa through 1 rotation and 3 GPa through 5 rotations at room temperature. In HPT, equivalent strain increases with distance from the center, so the effects of strain was compared to the solutionized material by

investigating the disks at several diameters, namely: at r=1 and r=5 mm on the 1 turn disk, and r=3.5mm on the 5 turn disk, corresponding to equivalent strains of ε=3, 16, & 57, respectively. Hardness was measured by Vickers indentation at 50gf, 15 second hold with a minimum of five indents at each location.

Plasma focused ion beam (PFIB, Thermo Fisher Scientific Helios Hydra UX) with Xe plasma was used to prepare atom probe tomography (APT) needles and to lift out transmission electron microscopy (TEM) foils from each location, within the most refined structure at each radius. Foils were thinned using a Ga-FIB and final polished in the PFIB with Xe to removed any residual Ga contamination. TEM (Thermo Fisher Scientific Titan Themis 300kV) was utilized to analyze the grain boundaries for solute segregation and atom probe tomography (Cameca Leap 4000 XHR) was used to quantify solute concentrations and visualize solute segregation morphologies at interfaces. APT analysis was conducted in voltage mode with a target evaporation rate of 0.005 atoms/pulse at a frequency of 200 kHz while specimens were maintained at 45K. APT results were reconstructed using Integrated Visualization and Analysis Software (IVAS).

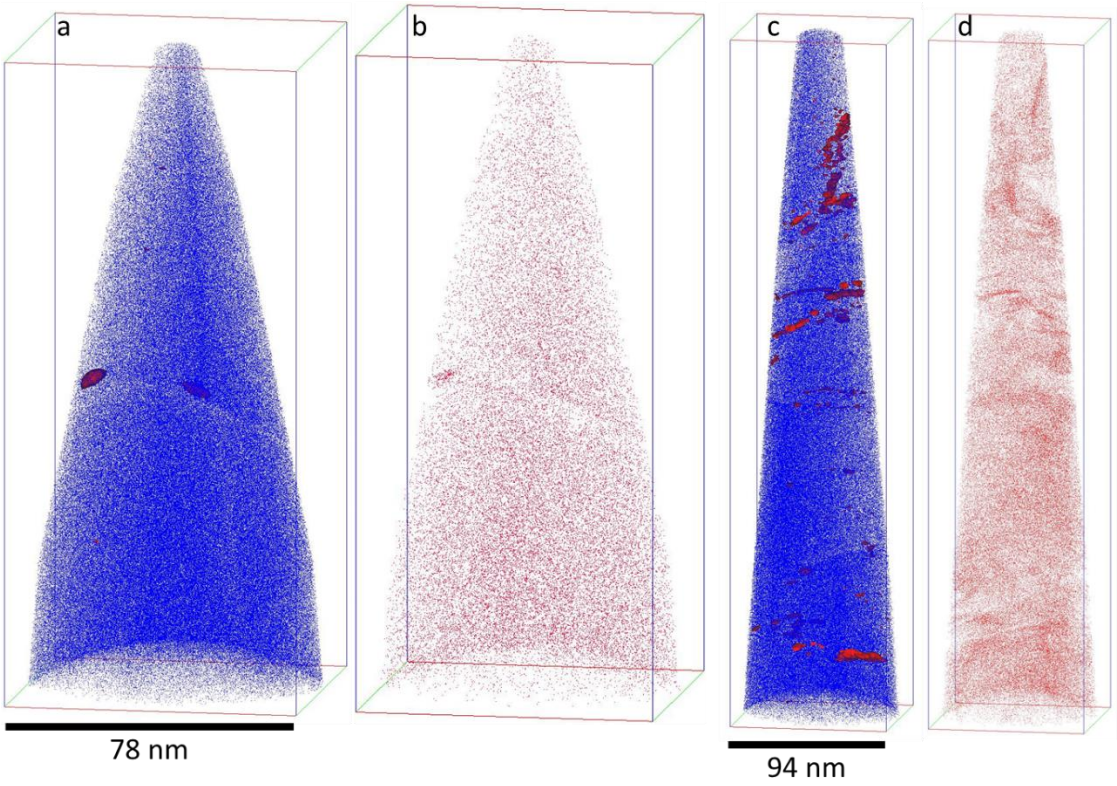

Figure 11. APT reconstructions of (a & b) the ε=16 and (c & d) ε=57 samples with (a & c) Mg ions and isosurfaces of 4 at% Y and (b & d) only Y containing species. (a) shows a grain boundary at half height with two obvious yttrium clusters and (c) shows very fine grains with many boundaries captured within the volume. Y is segregated into clusters at many of the boundaries, with localized depletion from the matrix.

3.3 Results and Discussion

The nanoscale elemental distribution of the solutionized material was investigated by APT and is shown in Fig. 1a & 1b. A homogenous distribution of yttrium throughout the reconstruction is observed, though no boundaries were captured within the evaporated volume. The yttrium concentration measured by APT is 0.58 at%, which is slightly less than the 0.82 at% measured by spark OES from the material supplier. The SEM (not shown)indicates a few small precipitates as well as YH_2 particles which were not completely dissolved during the solutionization treatment, but these are scant and make up

a very small portion of the total volume. Fig. 1c is the APT reconstruction of the needle lifted from r=1mm (ε=3) after processing through 1 turn of HPT. The Y species show no obvious segregation to the boundary, but when enlarging a 25nm thick slice of the top 255nm of the tip (Fig 1e). The coherency in the pole figures suggest that the boundary seen near the tip is a twin variant, with nominal yttrium enrichment in very small clusters (Fig. 1f). This agrees with Wang et al. who showed yttrium clusters at twin boundaries (TBs) after compression to 2% plastic strain, also in a Mg3Y alloy [5]. In both the Wang et al. work and this report, the annealed material was inspected and no clusters were observed.

At the higher strain of ε=16 (r=5 mm in the 1 turn disk), Fig. 2a shows a few small clusters of yttrium at boundaries, with one cluster at a triple junction. The Y remaining in the matrix remains reasonably consistent at this level of strain (Fig. 2b). Measuring the yttrium clusters at the 4 at% isosurface shows that even the largest clusters are less than 10nm, again aligning well with other literature on RE clusters in Mg where clusters are seen to be ~1-5nm [5], [7]. Three distinct boundaries were observed within this needle, all of which had at least a few clusters with increased yttrium concentration, though not all boundaries are visible in Fig. 2a due to single orientation depiction. In the highest strain condition investigated of ε=57 (5 turns, r=3.5) the solute shows increased segregation and, typical of HPT processing, the grain boundary spacing is on the order of 10s of nm within the APT reconstruction (Fig. 2d).

The differences between the 2% compression deformation-induced segregation and the HPT-induced ε=3 strain suggests that the segregation may occur under different defect pathways and/or at different diffusion rates under the high hydrostatic pressures and shear

strains present in HPT. Small amounts of thermal energy can be produced by HPT, however the temperature rise during straining is observed to be very small and thus thermally-enhanced diffusion during HPT is not suspected to contribute to segregation. Edalati found that the highest temperature rise in titanium processed at similar rotation speeds and to similar equivalent strains to be below 20°C [8]. A likely difference in segregation mechanisms between compression and HPT is that the latter creates a larger number of defects, including dislocation and vacancy concentrations that are above equilibrium levels [9]. The increase in free volume, combined with the large atomic misfit between Mg (0.160 nm) and Y (0.180 nm) favors enhanced transport of solutes within the material, ultimately leading to increased solute segregation and clustering.

Other reports on HPT processed Mg-1Nd-1Mn have shown similar segregation of Nd solutes, however the segregation reaches a maximum after 1 turn and does not change with further deformation [10]. In a Mg-7.6Zn-1.7Y (wt%) alloy processed by HPT at room temperature, Zn segregates as soon as the material was put under axial pressure, while the Y does not show any segregation even after 5 turns [11]. While the origins of these observations is not fully clear, it has been reported that ternary elements can modify the interfacial segregation kinetics of RE elements in Mg [12], and thus may be playing a role that might be explored in future studies. Further studies may also explore transitions where excess RE solute on grain boundaries results in embrittlement [13].

3.4 Conclusion

Ambient temperature strain induced segregation of yttrium to grain and twin boundaries has been reported, with increasing strain causing increased segregation in a Mg

3Y (wt%) alloy. HPT is expected to alter the segregation pathways through the generation of an excess of free volume and pipe diffusion in dislocations created by the hydrostatic confinement during processing. These findings point to the ability to tailor grain boundary segregation beneficial to the mechanical response via the application of large strain.

References

[1] J. D. Robson, S. J. Haigh, B. Davis, and D. Griffiths, "Grain Boundary Segregation of Rare-Earth Elements in Magnesium Alloys," *Metall. Mater. Trans. A*, vol. 47, no. 1, pp. 522–530, Jan. 2016, doi: 10.1007/s11661-015-3199-3.

[2] Z. Pei, R. Li, J.-F. Nie, and J. R. Morris, "First-principles study of the solute segregation in twin boundaries in Mg and possible descriptors for mechanical properties," *Mater. Des.*, vol. 165, p. 107574, Mar. 2019, doi: 10.1016/j.matdes.2018.107574.

[3] J. F. Nie, Y. M. Zhu, J. Z. Liu, and X. Y. Fang, "Periodic Segregation of Solute Atoms in Fully Coherent Twin Boundaries," *Science*, vol. 340, no. 6135, pp. 957–960, May 2013, doi: 10.1126/science.1229369.

[4] Z. Huang *et al.*, "Dislocation-induced Y segregation at basal-prismatic interfaces in Mg," *Comput. Mater. Sci.*, vol. 188, p. 110241, Feb. 2021, doi: 10.1016/j.commatsci.2020.110241.

[5] X. Wang *et al.*, "Room Temperature Deformation-induced Solute Segregation and its Impact on Twin Boundary Mobility in a Mg-Y Alloy," *Scr. Mater.*, vol. 209, p. 114375, Mar. 2022, doi: 10.1016/j.scriptamat.2021.114375.

[6] X. Sauvage, A. Duchaussoy, and G. Zaher, "Strain Induced Segregations in Severely Deformed Materials," *Mater. Trans.*, vol. 60, no. 7, pp. 1151–1158, Jul. 2019, doi: 10.2320/matertrans.MF201919.

[7] J. F. Nie, N. C. Wilson, Y. M. Zhu, and Z. Xu, "Solute clusters and GP zones in binary Mg–RE alloys," *Acta Mater.*, vol. 106, pp. 260–271, Mar. 2016, doi: 10.1016/j.actamat.2015.12.047.

[8] K. Edalati, Y. Hashiguchi, P. H. R. Pereira, Z. Horita, and T. G. Langdon, "Effect of temperature rise on microstructural evolution during high-pressure torsion," *Mater. Sci. Eng. A*, vol. 714, pp. 167–171, Jan. 2018, doi: 10.1016/j.msea.2017.12.095.

[9] B. Oberdorfer *et al.*, "Absolute concentration of free volume-type defects in ultrafine-grained Fe prepared by high-pressure torsion," *Scr. Mater.*, vol. 63, no. 4, pp. 452–455, Aug. 2010, doi: 10.1016/j.scriptamat.2010.05.007.

[10] P. C. de Oliveira, L. A. Montoro, M. T. Perez-Prado, A. Hohenwarter, R. B. Figueiredo, and A. Isaac, "Development of segregations in a Mg–Mn–Nd alloy during HPT processing," *Mater. Sci. Eng. A*, vol. 802, p. 140423, Jan. 2021, doi: 10.1016/j.msea.2020.140423.

[11] D. A. Basha, R. Sahara, H. Somekawa, J. M. Rosalie, A. Singh, and K. Tsuchiya, "Interfacial segregation induced by severe plastic deformation in a Mg–Zn–Y alloy," *Scr. Mater.*, vol. 124, pp. 169–173, Nov. 2016, doi: 10.1016/j.scriptamat.2016.07.021.

[12] H. Zhou *et al.*, "Effect of Ag on interfacial segregation in Mg–Gd–Y–(Ag)–Zr alloy," *Acta Mater.*, vol. 95, pp. 20–29, Aug. 2015, doi: 10.1016/j.actamat.2015.05.020.

[13] L. Xiao *et al.*, "Unexpected high-temperature brittleness of a Mg-Gd-Y-Ag alloy," *J. Magnes. Alloys*, p. S2213956721001638, Jul. 2021, doi: 10.1016/j.jma.2021.06.018.

Chapter 4 – Hall-Petch Strengthening in Nanocrystalline Concentrated Mg-RE Alloys

Suveen Mathaudhu[a,b,c]*, Christian Roach[a], Arun Devaraj[b]

[a]University of California, Riverside, USA

[b]Pacific Northwest National Laboratory, USA

[c]Colorado School of Mines, USA

*Corresponding author: smathaudhu@mines.edu, 1500 Illinois St., Golden, CO 80401

Abstract

Magnesium alloys with added dilute quantities of rare earth (RE) elements such as Y, Nd and Gd have shown increased strength, reduced texture anisotropy, increased grain size stability and low-temperature ductility. Many of these properties are a result of solute interactions along interfaces such as grain and coherent twin boundaries. Additional strengthening can be gained through refinement of the Mg-RE grains to the nanoscale regime by severe plastic deformation. In this work, we study the segregation of RE solutes during high-pressure torsion (HPT) processing of Mg-RE alloys. Empirical trends for grain size and hardness as a function of total solute concentration are presented, and point to increased grain refinement, grain size stabilization and strengthening with increasing solute content. Literature reports and experimental evidence for the HPT process driving excess solute to the nanocrystalline grain boundaries via solute drag, pipe-diffusion and vacancy diffusion are presented, along with Hall-Petch trends in comparison with pure Mg across a wide span of grain sizes from ~30 nm to 1000 μm. The findings here point to the lack of inverse Hall-Petch behavior resulting from RE solute stabilization of the grains against

grain boundary mediated softening. These results point to the use of large-strain processing towards grain boundary engineering of nanocrystalline Mg-RE alloys for enhanced mechanical behavior.

Keywords: nanocrystalline, magnesium, high-pressure torsion, rare earth, Hall-Petch

4.1 Introduction

Lightweight Mg alloys have been known to suffer from a lack of low temperature formability on account of their hexagonal close-packed structure, and limited number of concurrently active deformation mechanisms. [1] This, combined with the limited strength of Mg alloys compared to more conventional Fe- or Al-based structural materials has hindered more widespread acceptance of its usage in structural applications. A compelling solution to the problem of formability and strength lies in the addition of dilute quantities of rare-earth element (RE) solutes (e.g. Y [2–5], Gd [6] and Nd [5,7]), which, when segregated to boundaries, have shown the ability to increase strength [8,9], suppress grain and twin boundary migration [5,7,10–12], enhance interfacial bonding [10,13,14], and lessen the crystallographic texture [15–19]. First-principles simulations have also predicted the potency of RE solutes on the strengthening and ductilization in Mg alloys; these RE solutes are shown to possess large segregation energies and increase the ductility and critically resolved shear stress when residing on either $\{10\bar{1}2\}$ extension or $\{10\bar{1}1\}$ compression twin boundaries. [20]

The location of these specific solutes in the Mg lattices is inferred to be uniformly distributed [21–23], with the need to drive the solutes to interfaces. Recent studies implementing high-resolution electron microcopy and mapping have demonstrated the

periodic segregation of Gd and Zn to coherent twin boundaries after annealing; combinations of low-strain deformation followed by annealing have shown similar effects. [7,12,24] With atomistic simulations Huang et al. showed Y segregation to basal-prismatic (BP) interfaces in a Mg1Y alloy compressed to 2% plastic strain to generate $\{10\bar{1}2\}$ twins. [25] These simulations were validated in a later work by Wang et al. who show that room temperature deformation alone, with no added annealing step, is enough to force solute Y to CTB interfaces and basal-prismatic (BP) facets in a Mg3Y alloy cube compressed to 2% plastic strain. [26] Further, evidence for Y in dislocation cores is presented, along with experimental conditions and simulations validating the concept of Y solute stabilizing boundaries. Mechanistically, they report that the Y segregation on BPs and CTBs is driven by local lattice distortion. [26]

An alternative strategy towards concurrent strengthening and ductilization of Mg alloys has been grain size reduction. [27] The relationship that relates the grain size to the yield strength (s_y) is known as the Hall-Petch equation [28,29], which has been extensively empirically validated over the past ~70 years. [30,31] In more recent times, the concept of an "inverse" Hall-Petch relationship has emerged wherein the Hall-Petch slope inverts at some very fine (10–100 nm) grain size in fcc materials, corresponding to a change in deformation physics from slip-based flow to grain boundary rotation or sliding. [27,32] In pure Mg, this has been shown to occur in the range of ~1–4 μm [33,34], with grain sizes in this region showing excellent combinations of strength and ductility. [33,35] A common path to refining grains to this range is through severe plastic deformation (SPD) methods, such as high-pressure torsion (HPT). [36–38] HPT imparts a large amount of shear strain

into a small disk confined under a pseudo-hydrostatic high-pressure state that minimizes failure via localization or fracture. The high number of dislocations that are produced energetically from cellular structures that convert to low- and then high-angle grain boundaries, with grain sizes typically less than 100 nm. [39]

A question then arises on how RE segregation proceeds under large strain deformation processing, such as HPT. de Oliveira et al. [40] observed substantial segregation of Nd to grain boundaries in the very early stages of HPT (1 turn) of a Mg1Nd1Mn (wt%) alloy. Increased Nd segregation to all boundaries, independent of their misorientation was observed with increased HPT turns. The Mn, which was in the form of small particles, fragmented into nanoparticles and individual solutes which also segregated to boundaries; however, the diffusion was more sluggish than the Nd, and the Mn clusters and solute were reported to not contribute to changes in hardness. The authors attribute the segregation of Nd to dislocation dragging of solutes to grain boundaries and/or solute dragging by moving grain boundaries.

To summarize, RE elements, when located on interfaces and boundaries have been shown to simultaneously increase strength and ductility. Both low-strain and high-strain deformation at ambient temperature have shown the ability to enhance RE segregation to boundaries, however the effects of the solutes, especially when residing along nano-crystalline grain boundaries, is much less investigated. With this in mind, this work will explore the role of RE elements on grain refinement and strengthening in Mg-RE alloys fabricated by HPT. The study includes extensive comparisons with literature reports of HPT-processed Mg-RE alloys, and the generation of extended Hall-Petch plots that cover

the range of grain sizes from the conventional course-grained regimes down to 10s of nanometers.

4.2 Materials and Methods

The starting material for this study was an as-cast binary Mg-3Y (wt%) alloy (Mg3Y) (Terves Inc Euclid, OH, USA). The as-cast material consisted of large (mm-scale) grains with clear Y-rich dendritic networks, and both $Mg_{24}Y_5$ and YH_2 precipitates, as shown in Fig. 1a. To dissolve the Y into solution, the alloy was solution annealed at 550°C for 12 hours in a tube furnace under positive argon atmosphere (0.02 MPa gauge), followed by water quenching to maintain the Y in solution. Fig. 1b shows the microstructure with no evidence of the prior dendritic networks, and a few small cuboidal YH_2 particles.

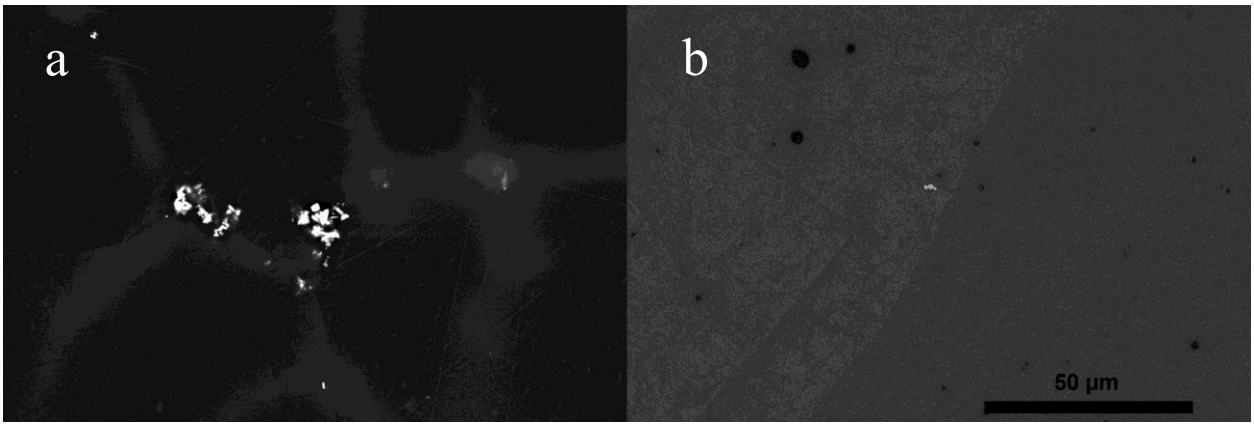

Figure 12. (a) Backscatter SEM image of as-cast Mg3Y showing Y-rich dendritic networks and $Mg_{24}Y_5$ and YH_2 precipitates and (b) backscattered SEM image of the solutionized Mg3Y showing no obvious Y-rich dendritic networks and a minimal presence of remaining YH_2 particles.

The solutionized and unsolutionized materials were cut into thin sheets (1.2mm thick) from which ø10mm discs were punched. Alloys were processed in both the as-received, unsolutionized state (4-turn, 3GPa, ~1.5 rpm) and in the solutionized state (5-

turn, 3GPa, ~1.5 rpm). While the samples were rotated to a different number of turns, sample selection was made from radii with equivalent strains typical of microstructural saturation and a uniform smallest average grain size (e > 20). [37] The remainder of the data set used for this study was selected from the extant literature on UFG and NC Mg-RE alloys processed by high-pressure torsion (Table 1). To focus on the role of RE solutes, simple binary or ternary RE-containing alloys were selected, and to minimize the role of precipitation hardening mechanisms, only reports on alloys HPT-processed at ambient temperatures after solutionization heat treatments and with no post-processing ageing treatment are cited. Powder metallurgy Mg alloys were excluded based on the presence of impurity solutes affecting microstructural evolution and resultant strength properties. Other than the Mg22.4Gd alloy [41], the surveyed alloys fall below the room temperature solubility limits (<1 at%) shown in the Mg-Nd [42], Mg-Y [43] and Mg-Gd [44] phase diagrams, Two data points for unalloyed Mg (99.9% [37] and 99.8% [45] purity) processed by HPT are also added, with care to include references where no self-annealing or grain growth had been observed.

Microstructural homogeneity was studied with a scanning electron microscope (SEM) (FEI Nova Nano 450). Grain sizes on the Mg3Y were measured via transmission electron microscopy (TEM) (FEI Titan Themis 300 at 300 kV). Microhardness (Phase II Micro Vickers Indenter) was measured using a load of 50gf for 15 s with data reported for at least 10 indents. Yield strengths in each alloy were approximated using Tabor's relationship:

$$\sigma_y(MPa) = \frac{HV\left(\frac{kgf}{mm^2}\right) * 9.81\left(\frac{m}{s^2}\right)}{3} \quad \text{Eq. 1}$$

Where σ_y is yield strength in MPa and *HV* is the Vickers hardness number in kgf/mm^2.

Atom probe tomography (APT) was performed on Ga-focus-ion beam (FIB) and plasma-FIB prepared needles in a Cameca LEAP 4000 XHR system at a temperature of 45K, running in voltage mode with a pulse frequency of 20% at 200kHz. APT data was reconstructed and analyzed using the Integrated Visualization and Analysis Software (IVAS) package.

Table 3. Literature reports and new material data for nanocrystalline Mg-RE alloys and baseline unalloyed nanocrystalline Mg

Alloy (wt%)	c [wt%]	c [at%]	d_{avg} [nm]	HV [kgf/mm^2]	σ_y [MPa]	Ref
Pure_Mg (99.9)	0.10	0.10	1000	35	114	[46]
Pure_Mg (99.8)	0.20	0.20	600	55	180	[47]
Mg-1.43Nd	1.43	0.24	600	79	258	[48]
Mg-1.1Y	1.10	0.30	230	68	222	[11]
Mg-1Nd-1Mn	2.00	0.62	200	77	252	[40]
Mg-3.6Nd	3.60	0.63	200	86	281	[49]
Mg-3Tb2Nd	4.90	0.81	100	110	360	[50]
Mg-3Y	3.00	0.82	100	87	284	This work
Mg-3Y*	3.00	0.82	300	63	206	This work
Mg-10Gd	10.00	1.70	58	107	350	[51]
Mg-22.4Gd	22.40	4.27	30	142	464	[41]

* Unsolutionized HPT-processed Mg3Y

4.3 Results

Fig. 2 presents TEM images of both the unsolutionized and solutionized materials after HPT processing to strains of e > 20 where a minimum grain size is achieved. The microstructure for Fig. 2a indicates that after HPT processing, the unsolutionized Mg3Y has grains averaging ~300 nm. Fig. 2b shows the same material after a solutionization heat

treatment. The addition of the solutionization step results in a much smaller grain size after deformation processing (~100 nm).

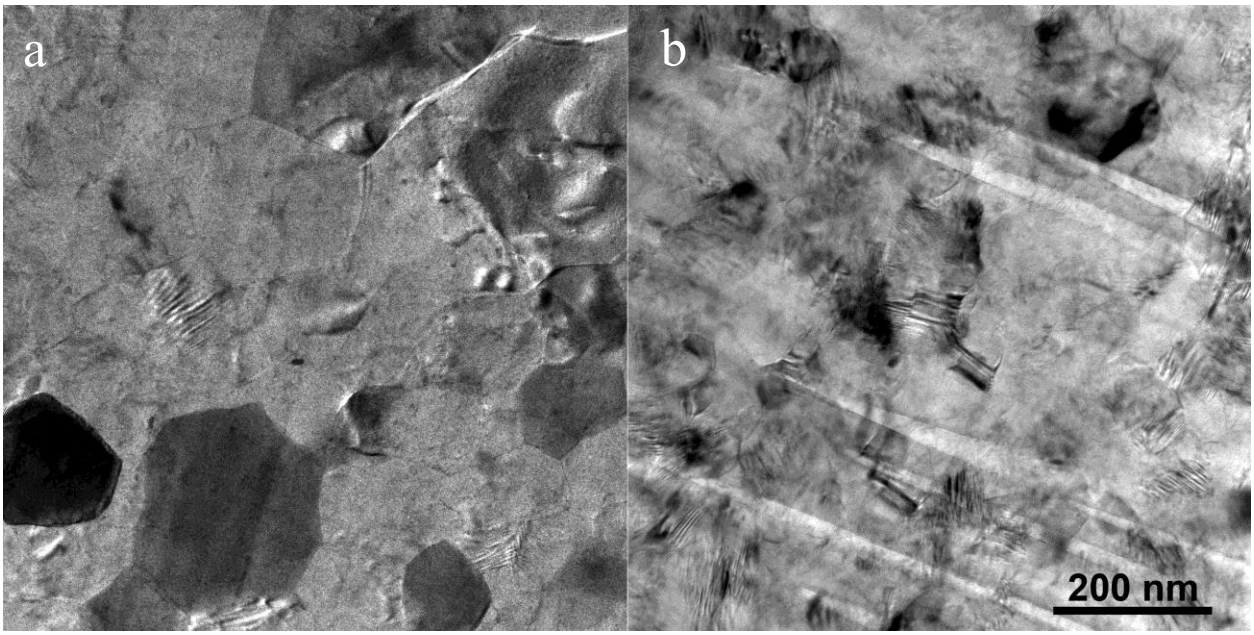

Figure 13. TEM images showing the effect of pre-processing solutionization in Mg3Y: (a) unsolutionized materials with d_{avg} = 300 nm and (b) solutionized material with d_{avg} = 100 nm.

Fig. 3 shows the average grain size (d_{avg}, left y-axis) of the materials in Table 1 as a function of total solute content (c, wt%). This data follows similar trends, i.e. a decrease in the average grain size proportional to the wt% of solutes in the alloy, to those reported by Cáceres and Rovera [52] for coarse-grained (grain sizes from ~90 μm to ~325 μm) Mg-Al alloys, however at much smaller grain sizes (crystallite sizes from ~50 nm to ~1000 nm). Akthar and Teghtsoonian [53] studied the solid solution strengthening mechanisms in Mg-Al alloy single crystals oriented for basal slip and found that the strengthening was attributed to basal plane hardening by the Al solutes. Cáceres and Rovera [52] suggested that this finding was the same strengthening mechanisms observed in their studies. This trend is also demonstrated by the difference is grain size for the HPT processed Mg3Y with

different pre-HPT processing microstructures (solutionized versus unsolutionized). The additional solutionized Y provides for a higher volume fraction to pin grains, and therefore a smaller grain size (Fig. 2). For the solutionized and processed UFG and NC regime, the grain size dependence on the total solute concentration (wt%) produces the empirical formula:

$$d_{avg} = 285 \cdot c^{-0.625} \quad \text{Eq. 2}$$

Where d_{avg} is the average grain size in nm and c is the solute content in wt%.

The secondary (right) y-axis on Fig. 3 gives the yield strength (σ_y) estimated with Eq. (1) as a function of solute concentration (wt%). A logarithmic relationship:

$$\sigma_y\ (MPa) = 57 \cdot \ln(c) + 239 \quad \text{Eq. 3}$$

that approaches saturation at σ_y ~ 450 MPa. The difference between the solutionized and unsolutionized Mg3Y on this graph demonstrates the role of solute in solution; the Y contained in the remnant precipitate fragments does not contribute to a smaller average grain size nor the associated strengthening seen in the solutionized Y.

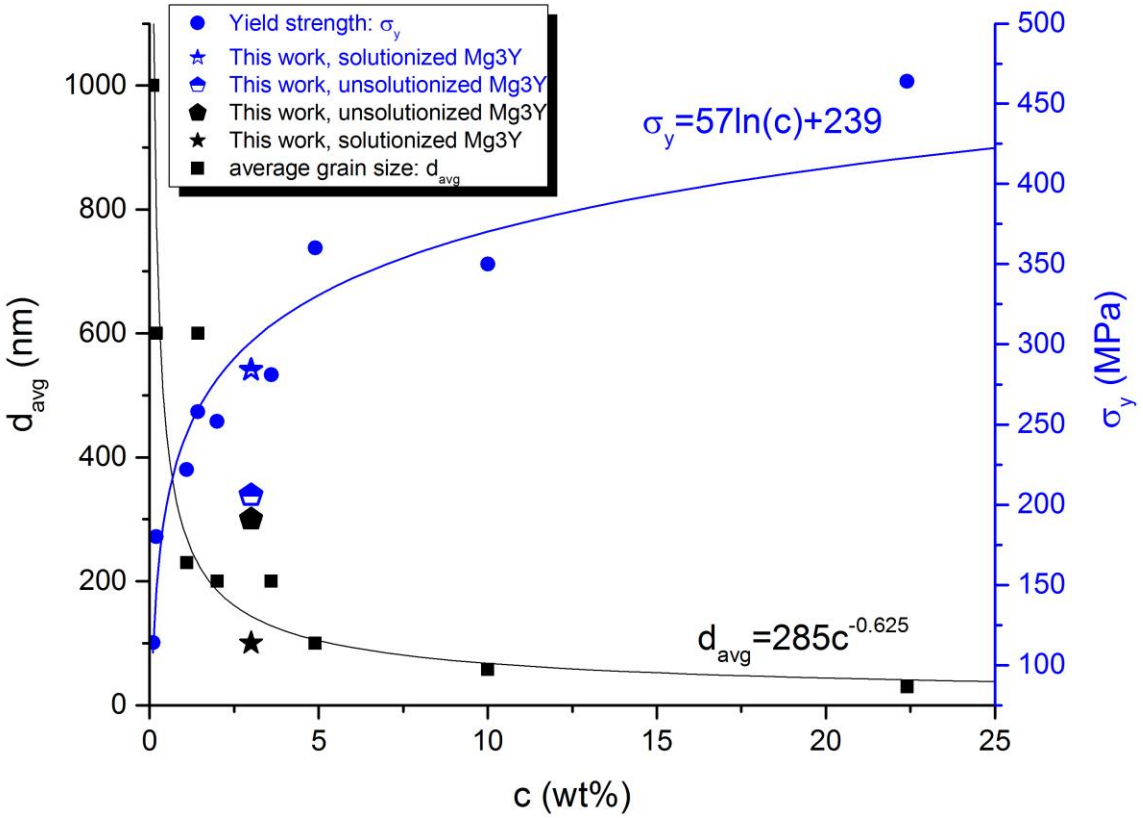

Figure 14. Smallest average grain size after HPT processing (d_{avg}) (left y-axis) and yield strength (s_y) predicted from Vickers hardness values (right y-axis). The stars and pentagons represent the solutionized and unsolutionized initial states, respectively. The data in the plot is aggregated from Table 1.

4.4 Discussion

The data from Fig. 3 suggests decreasing grain size as a function of increased solute concentration. Y.C. Lee et al. reported similar observations for binary Mg-X (X = Al, Zr, Ca) alloys fabricated by solidification, and attribute the enhanced refinement to the growth restriction effects caused by constitutional undercooling during solidification and the alloy effect as nucleating particles (or secondary phases). [54] They similarly observed the grain size approaching a constant value at higher levels of solute additions. While fundamentally playing the same role of restricting grain boundary migration, the mechanisms by which solutes are reported to contribute to grain refinement are quite different for deformation-

induced processing, such as HPT. Edalati et al. studied a number of pure and binary solid-solution alloys processed by HPT. [55] As a caveat, the explored systems were all bcc or fcc, and none of the solute atoms were rare-earth elements. They also observed a decrease in steady-state grain size, and increases in hardening/strengthening with increasing alloy content, in all systems probed. Their finding was that the effects of solute-matrix atomic mismatch and modulus interactions on edge dislocations were the primary factor promoting grain refinement. In other words, the solute atoms increase the local stress needed for a dislocation to move, and therefore hinder dislocation recovery and grain boundary migration, encouraging the formation of smaller dislocation cells that convert to nanocrystalline (NC) grains with high angles, typical of SPD processing. [39] The trends displayed in Fig. 3 for NC Mg-RE alloys would appear to be consistent with those of Edalati et al. [55], and are further supported by the large atomic mismatch between the Mg lattice (0.160 nm) and the similar large metallic radii of the studied rare earth elements: Nd (0.181 nm), Gd (0.180 nm), Tb (0.177 nm) and Y (0.180 nm).

Edalati et al. also suggest that grain size hardening plays the strongest role on strengthening, with the solid-solution contribution to hardening being less than 15% of the total. [55] This is in contrast to the work reported on coarse-grained Mg-Al alloys [52], where the solid solution contribution to strengthening is reported to be quite high:

$$\sigma_{ss}(MPa) = CX^n \qquad \text{Eq. 4}$$

where σ_{ss} is the solid solution strengthening in MPa, *C is a constant* =197 MPa in this case, *X* is the atomic concentration of Al and *n* is the exponential factor in the range of 1/2 ~ 2/3, -2/3 used here. [52,56] While this analysis was derived for smaller solutes (Al (0.143nm)

and Zn (0.134nm)), Akhtar and Teghtsoonian suggest that this should be a general solutions effect based on data for Al and Zn, but also Pb (0.180nm), In (0.167nm) and Cd (0.151nm). [53] Applying this equation to the dataset in Table 1 (other than the unalloyed pure Mg) with either n=½ or n=2/3, the lowest contribution to the total Tabor estimated yield strength is 29% in the Mg1.43Nd (0.24 at%, n=2/3) and the highest is above 100% for the Mg22.4Nd (4.27 at%, n=2/3). These estimates of solid solution strengthening are quite high, especially given the expected role of grain boundary strengthening provided by the NC grains. The expected source of this overprediction of solid solution strengthening in nanograined Mg-RE alloys produced by large-strain deformation will be addressed.

Fig. 4 presents an APT reconstruction of the solutionized Mg3Y alloy after HPT processing (3 GPa, 5-turns, ε=57). During FIB preparation, the Ga ions (shown in yellow) have high diffusivity [57] and preferentially located along grain boundaries, thereby providing a marker useful for grain boundary identification. The spacing of the boundaries is consistent with the TEM grain size analysis (d_{avg}≈100 nm) in Fig. 2b. From this reconstruction, it is clear that Y segregates in large quantities along grain boundary interfaces. This volume and pattern of Y segregation matches the observations of Nd segregation to all boundaries during HPT processing of Mg1Nd1Mn [40], and visibly exceeds the content of solutes observed on CTBs by annealing [12] or small-strain compression deformation of Mg3Y [26].

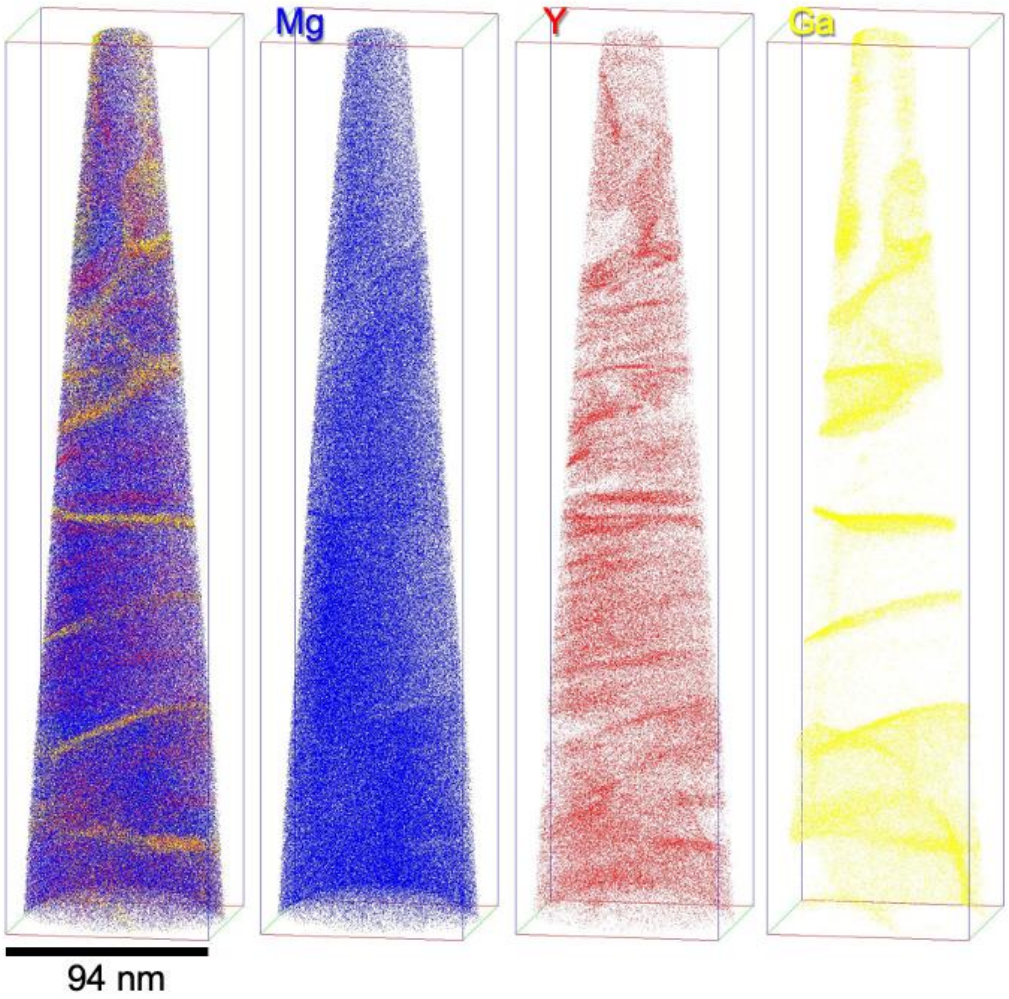

Figure 15. APT reconstruction of the Mg3Y HPT processed at 3 GPa and 5 turns, from a radius corresponding to a ε=57. The species color corresponds to Mg (blue), Y (red), and Ga (yellow).

Recall that in the study by Wang et al. on compressed Mg3Y, segregation was driven to dislocation cores at CTBs, as well as BP interfaces. [26] This suggests that solutes may be driven to any meta-stable dislocation structure, based on the hydrostatic tensile stresses alone. At much larger strains, de Oliviera et al. posit diffusion by dislocation dragging and grain boundary dragging. [40] Sauvage et al. have suggested many possible segregation mechanisms for severely deformed materials, typically processed by SPD. [58]

They propose that SPD-processed materials are typified as having high dislocation densities, “non-equilibrium” grain boundaries, and high vacancy concentrations, which may all lead to different pathways for solute mobility. They show that room temperature atomic mobility can be increased by several orders of magnitude under SPD conditions, and attribute strain-induced vacancies as playing a key role in activating grain boundary segregation during SPD, but in the early stages of processing (viz. low-strain), solute drag by moving boundaries provides the key mechanism for grain boundary segregation. [59,60] Given the dynamic nature of defect evolution and grain formation during the HPT process, it is reasonable that the solute segregation mechanisms will also dynamically evolve as the microstructure does, and while not the focus of this study, the topic does merit additional exploration.

The Hall-Petch equation is typically given in the form:

$$\sigma_y = \sigma_0 + kd^{-\frac{1}{2}} \qquad \text{Eq. 5}$$

Where σ_y is the yield strength, σ_o is the frictional stress, k is a stress concentration factor and d is the grain size. While a variety of physics can explain the Hall-Petch relationship [30–32], the k value can be characterized as the magnitude of resistance of the grain boundary to slip propagation. For Mg and it’s alloys, this value can span a wide range of values based on crystallographic texture, grain size, grain boundary characteristics, temperature and strain. [61] In pure Mg the Hall-Petch trend has been reported to incur a number of inflections in slope corresponding to fundamental changes in the underlying deformation mechanisms, including the observation of a inverse Hall-Petch slope in the grain size range of 1-4 μm. [33,34] Fig. 5 presents such data from Zheng et al. [33], with

the *k* value for Region I (k = 260 MPa/mm^2) being representative of twin-dominated deformation, as is common for in coarse-grained Mg and its alloys (k_{Mg} = 294 MPa/mm^2, k_{Mg1Zn} = 273 MPa/mm^2, k_{Mg1Y} = 252 MPa/mm^2) [62]. Region II extends from grain sizes of 1.57 to 5.32 μm and has a smaller k-value (88 MPa/mm^2) which is indicative of suppression of twinning to the point of slip becoming the dominant deformation mechanism, with some contributions from twinning, and possibly from grain boundary sliding. Region III (grain size <1.57 μm) has a negative k value, indicating strain softening due to grain boundary sliding and/or rotation dominating strain accommodation. Processing of pure Mg in Regions II and III has resulted in prominent room-temperature plasticity and homogenous flow, atypical of Mg alloys which are commonly textured, giving strongly anisotropic flow properties. [35,63,64] Also show in Fig. 5 is data on pure Mg collected from Cordero et al. [30] which also has been parsed into three regions: Region I (grain size >10 μm), Region II (grain size from 1.00 μm to 10 μm) and Region III (grain size <1.57 μm). The *k* values from Region I (k = 279 MPa/mm^2) agree very well with the data from Zheng et al. [33] and Somekawa and Mukai [62], with Region II also showing a similar k-value, indicating the reduction of twin activity, and increased slip and grain boundary mediated activity. However, unlike many previous publications, the Cordero et al. [30] data does not display in inversion in k for Region III, and neither does the data plotted for the nanocrystalline Mg-RE alloys studied herein.

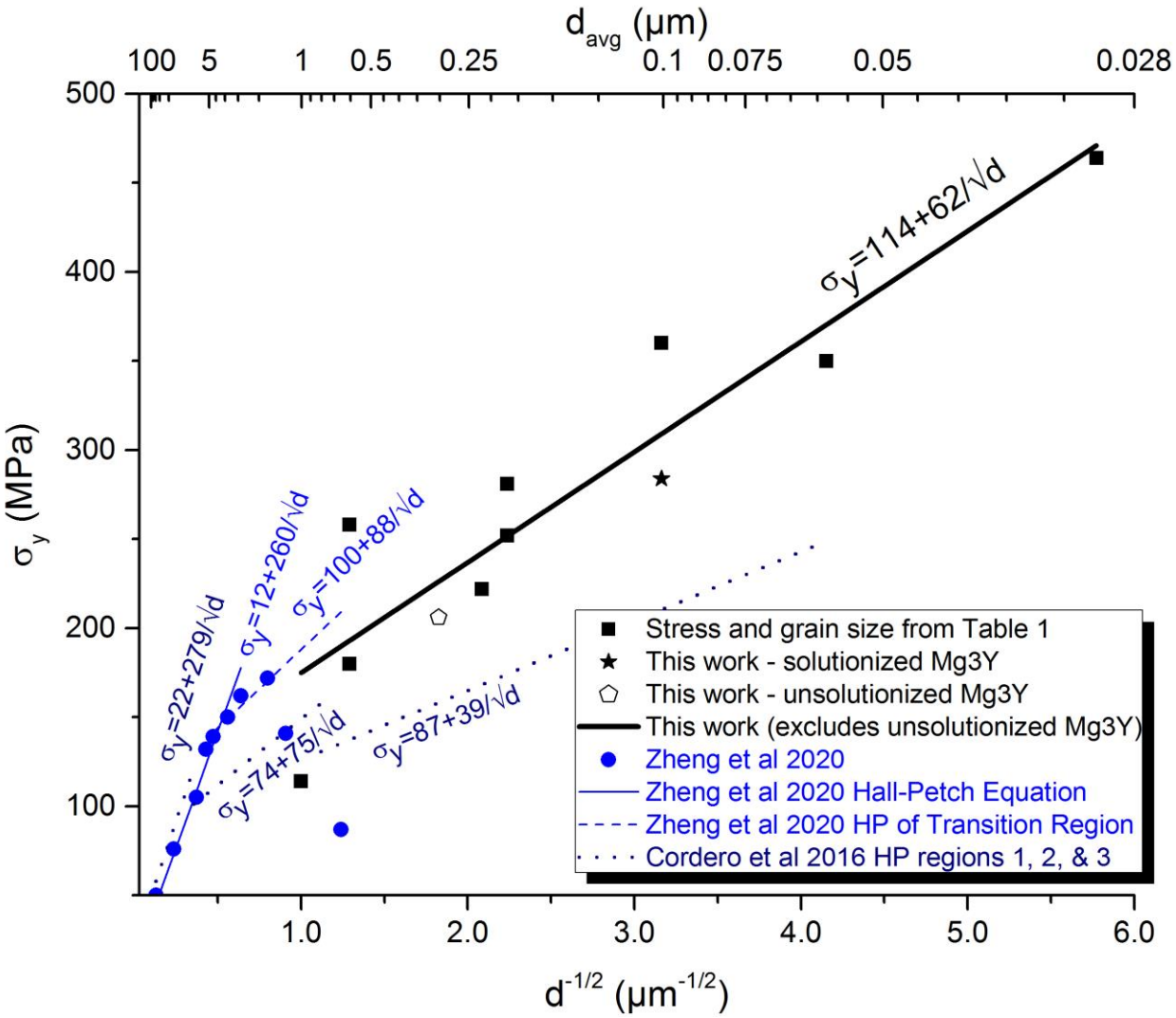

Figure 16. Hall-Petch relationships assembled from data in Table 1 for HPT processed nanocrystalline Mg-RE alloys, pure Mg processed by HPT [33] and pure Mg reported across the literature [30] with the exception of [33].

Careful review of the data used for Cordero et al. [30] Region III indicates that, of the six data points used to generate the trendline, three data points were from ball-milled and extruded powders [65], implicating the role of impurities in pinning an stabilizing grain boundaries against sliding, and one data point from a thin-film processed UFG (250 nm thick) Mg [66], with reported amorphous oxide pockets randomly dispersed between the

grains, again implicating extrinsic mechanisms that prevent grain boundary mediated deformation. The trendlines from the nanocrystalline Mg-RE alloys also do not display any inverse Hall-Petch response down to ~30 nm grain sizes, and more so, despite being alloyed with various concentration of RE solutes, the k-value suggests a continuation of the Region II trend, predicting mixed contributions from non-basal slip, and minimal, if any contributions of grain boundary sliding to the plasticity given the presence of the segregated solutes. It is also speculated that the segregation of RE solutes to grain boundaries during the HPT synthesis results in a RE-rich grain boundary, and a RE-depleted core with greater stabilization against grain growth via Zener pinning with solute clusters [67] or individual segregated solutes[68]. This also is the speculated reason for the overprediction of solution strengthening from Eq. (5); excess solute segregated to a grain boundary increases the "strength" of that grain boundary, while decreasing the lattice-straining role played by the large RE solutes in solution.

The k-value for the nanocrystalline Mg-RE ($k = 62$ MPa/mm^2) is slightly higher in Region III of the Cordero et al. data [30] ($k = 39$ MPa/mm^2), indicating a stronger resistance to dislocation slip in the Mg-RE nanocrystalline materials. However, the trends observed between the pure Mg and the Mg-RE alloys in the < 1μm region do agree with the data from Somekawa and Mukai [62] showing similar k-values, but increasing s_0 values for alloys with increased solute content. It is speculated that the presence of segregated RE solutes to the grain boundaries results in an increased critical stress needed to nucleate dislocations, thereby increasing the yield strength compared to pure Mg at equivalent grain sizes. [69] Recall that Akthar and Teghtsoonian [53] and Cáceres and Rovera [52] both

cited that the increase in strength due to solutes stemmed from the increase stress resistance created by the solutes on the basal plane. This observation can be extrapolated to apply to the non-basal <c+a> slip modes expected in this region. [70] Given the large amount of solute segregated to grain boundaries, it is unsurprising that the observed Hall-Petch trends for the nanocrystalline Mg-RE are also represented by "core-and-mantle" grain models, where a composite grain consists of a "core" interior, and a work-hardened "mantle" where segregation has occurred. [71,72] This relationship has been shown to be in excellent agreement with the Hall–Petch dependence for micrometer-sized grains, but predict reduction in slope for smaller grain sizes [27], as observed in Fig. 5.

Energetically and geometrically, the large RE solutes will favor regions of extended free volume, such as high angle grain boundaries typical of SPD processed materials. Lattice distortion is minimized in these circumstances. And while it is often argued that the large atomic radii of RE solutes provide the mechanisms for improved strength properties, *ab initio* simulations suggest that RE solutes have a unique electronic structure in the outer electron orbital that favors enhanced bonding with grain boundaries, resulting in a stronger bond with grain boundaries than other solutes, which affects grain boundary energy, cohesion and mobility. These mechanical properties such as yield strength and ductility, nor textural modification were studied here, however the local effects of RE solute atoms on grain boundaries, along with mechanistic connections to mechanical property changes are ripe for exploration. Severe plastic deformation methods offer an intriguing approach to control the segregation of solutes to various boundaries and reveal the limits of mechanical property improvements achievable.

4.5 Conclusion

Experiments and literature data for solutionized Mg-RE alloys processed via ambient temperature high-pressure torsion were collected and analyzed for trends relating the solute content to average processed ultrafine or nanocrystalline grain size, hardening and strengthening contributions. These findings suggest the possibility of using deformation for engineering grain boundary chemistry in nanocrystalline Mg alloys for simultaneous stability and strength. The following results were observed:

(1) A reduction in average grain size, and correspondingly, increases in yield strength with increasing solid solution solute content matches trends reported in literature for coarse-grained Mg-alloys. This trend is a result of solute strengthening of basal plane slip, and stabilization of fine grain boundaries through strain-driven segregation.

(2) Contrary to literature findings, the Hall-Petch plot does not demonstrate an inversion or even a major decrease in k in the grain size regime below ~ 1μm, which is reportedly due to the transition from twinning and slip-dominated deformation to activation of grain boundary sliding and rotation mechanisms. Instead, the slope generally follows the behavioral trends of unalloyed Mg in a region where there are mixed contributions from non-basal dislocation slip mechanisms.

(3) The root cause of the increasing linear continuation of the Hall-Petch trend for nanocrystalline Mg-RE alloys is attributed to literature reports and APT observations of the segregation of RE atoms to grain boundary interfaces under the large-strain deformation conditions provided by HPT. In turn, these solutes serve

to both stabilize grain boundaries against growth while simultaneously limiting the grain boundary sliding or rotation to which the inverse Hall-Petch behavior in ultrafine-grained pure Mg is commonly attributed.

Declaration of Competing Interest

The authors declare that they have no known competing financial interests or personal relationships that could have appeared to influence the work reported in this paper.

Acknowledgements

CJR and SNM were supported in part via the US National Science Foundation grant #1463679.

CJR was hosted at the US Department of Energy's (DOE) Pacific Northwest National Laboratory via support from a DOE Office of Science Graduate Student Research (SCGSR) Program Fellowship. AD would like to acknowledge the laboratory directed research and development (LDRD) funding as a part of Solid Phase Processing Science Initiative (SPPSi) from Pacific Northwest National Laboratory.

References

[1] T.M. Pollock, Weight loss with magnesium alloys, Science. 328 (2010) 986–987. https://doi.org/10.1126/SCIENCE.1182848.

[2] S.R. Agnew, M.H. Yoo, C.N. Tomé, Application of texture simulation to understanding mechanical behavior of Mg and solid solution alloys containing Li or Y, Acta Mater. 49 (2001) 4277–4289. https://doi.org/10.1016/S1359-6454(01)00297-X.

[3] S. Sandlöbes, M. Friák, J. Neugebauer, D. Raabe, Basal and non-basal dislocation slip in Mg–Y, Mater. Sci. Eng. A. 576 (2013) 61–68. https://doi.org/10.1016/J.MSEA.2013.03.006.

[4] Z. Wu, W.A. Curtin, The origins of high hardening and low ductility in magnesium, Nature. 526 (2015) 62–67. https://doi.org/10.1038/nature15364.

[5] J.D. Robson, S.J. Haigh, B. Davis, D. Griffiths, Grain Boundary Segregation of Rare-Earth Elements in Magnesium Alloys, Metall. Mater. Trans. Phys. Metall. Mater. Sci. 47 (2016) 522–530. https://doi.org/10.1007/s11661-015-3199-3.

[6] Y.M. Zhu, S.W. Xu, J.F. Nie, {101¯1} Twin boundary structures in a Mg–Gd alloy, Acta Mater. 143 (2018) 1–12. https://doi.org/10.1016/J.ACTAMAT.2017.09.067.
[7] X. Zhao, H. Chen, N. Wilson, Q. Liu, J.F. Nie, Direct observation and impact of co-segregated atoms in magnesium having multiple alloying elements, Nat. Commun. 10 (2019) 1–7. https://doi.org/10.1038/s41467-019-10921-7.
[8] A. Kula, X. Jia, R.K. Mishra, M. Niewczas, Mechanical Properties of Mg-Gd and Mg-Y Solid Solutions, Metall. Mater. Trans. B Process Metall. Mater. Process. Sci. 47 (2016) 3333–3342. https://doi.org/10.1007/s11663-015-0565-x.
[9] A. Kula, X. Jia, R.K. Mishra, M. Niewczas, Flow stress and work hardening of Mg-Y alloys, Int. J. Plast. 92 (2017) 96–121. https://doi.org/10.1016/J.IJPLAS.2017.01.012.
[10] H. Somekawa, S. Ogata, N. Tsuji, Mechanical Properties and Deformation Sizes Grain size, (2017). https://doi.org/10.1007/978-3-319-52392-7.
[11] R. Zheng, I. Kawarada, W. Gong, A. Shibata, H. Somekawa, S. Ogata, N. Tsuji, Effect of grain size on mechanical properties of mg-0.3at.%y dilute alloy, Mater. Sci. Forum. 941 MSF (2018) 790–795. https://doi.org/10.4028/www.scientific.net/MSF.941.790.
[12] J.F. Nie, Y.M. Zhu, J.Z. Liu, X.Y. Fang, Periodic segregation of solute atoms in fully coherent twin boundaries, Science. 340 (2013) 957–960. https://doi.org/10.1126/science.1229369.
[13] R. Mahjoub, N. Stanford, The electronic origins of the “rare earth” texture effect in magnesium alloys, Sci. Rep. 11 (2021) 1–9. https://doi.org/10.1038/s41598-021-93703-w.
[14] T. Tsuru, H. Somekawa, D.C. Chrzan, Interfacial segregation and fracture in Mg-based binary alloys: Experimental and first-principles perspective, Acta Mater. 151 (2018) 78–86. https://doi.org/10.1016/J.ACTAMAT.2018.03.061.
[15] T. Al-Samman, X. Li, Sheet texture modification in magnesium-based alloys by selective rare earth alloying, Mater. Sci. Eng. A. 528 (2011) 3809–3822. https://doi.org/10.1016/J.MSEA.2011.01.080.
[16] K. Hantzsche, J. Bohlen, J. Wendt, K.U. Kainer, S.B. Yi, D. Letzig, Effect of rare earth additions on microstructure and texture development of magnesium alloy sheets, Scr. Mater. 63 (2010) 725–730. https://doi.org/10.1016/J.SCRIPTAMAT.2009.12.033.
[17] B.Q. Shi, R.S. Chen, W. Ke, Effects of yttrium and zinc on the texture, microstructure and tensile properties of hot-rolled magnesium plates, Mater. Sci. Eng. A. 560 (2013) 62–70. https://doi.org/10.1016/J.MSEA.2012.09.010.
[18] N. Stanford, Micro-alloying Mg with Y, Ce, Gd and La for texture modification—A comparative study, Mater. Sci. Eng. A. 527 (2010) 2669–2677. https://doi.org/10.1016/J.MSEA.2009.12.036.
[19] N. Stanford, D. Atwell, A. Beer, C. Davies, M.R. Barnett, Effect of microalloying with rare-earth elements on the texture of extruded magnesium-based alloys, Scr. Mater. 59 (2008) 772–775. https://doi.org/10.1016/J.SCRIPTAMAT.2008.06.008.

[20] Z. Pei, R. Li, J.F. Nie, J.R. Morris, First-principles study of the solute segregation in twin boundaries in Mg and possible descriptors for mechanical properties, Mater. Des. 165 (2019) 107574. https://doi.org/10.1016/j.matdes.2018.107574.
[21] A. Tehranchi, B. Yin, W.A. Curtin, Solute strengthening of basal slip in Mg alloys, Acta Mater. 151 (2018) 56–66. https://doi.org/10.1016/J.ACTAMAT.2018.02.056.
[22] M. Ghazisaeidi, L.G. Hector, W.A. Curtin, Solute strengthening of twinning dislocations in Mg alloys, Acta Mater. 80 (2014) 278–287. https://doi.org/10.1016/J.ACTAMAT.2014.07.045.
[23] J.A. Yasi, L.G. Hector, D.R. Trinkle, First-principles data for solid-solution strengthening of magnesium: From geometry and chemistry to properties, Acta Mater. 58 (2010) 5704–5713. https://doi.org/10.1016/J.ACTAMAT.2010.06.045.
[24] N. Stanford, G. Sha, J.H. Xia, S.P. Ringer, M.R. Barnett, Solute segregation and texture modification in an extruded magnesium alloy containing gadolinium, Scr. Mater. 65 (2011) 919–921. https://doi.org/10.1016/J.SCRIPTAMAT.2011.08.012.
[25] Z. Huang, V. Turlo, X. Wang, F. Chen, Q. Shen, L. Zhang, I.J. Beyerlein, T.J. Rupert, Dislocation-induced Y segregation at basal-prismatic interfaces in Mg, Comput. Mater. Sci. 188 (2021) 110241. https://doi.org/10.1016/j.commatsci.2020.110241.
[26] X. Wang, Y. Hu, K. Yu, S. Mahajan, I.J. Beyerlein, E.J. Lavernia, T.J. Rupert, J.M. Schoenung, Scripta Materialia Room Temperature Deformation-induced Solute Segregation and its Impact on Twin Boundary Mobility in a Mg-Y Alloy, 209 (2022). https://doi.org/10.1016/j.scriptamat.2021.114375.
[27] M.A. Meyers, A. Mishra, D.J. Benson, Mechanical properties of nanocrystalline materials, Prog. Mater. Sci. 51 (2006) 427–556. https://doi.org/10.1016/j.pmatsci.2005.08.003.
[28] E.O. Hall, Yield Point Phenomena in Metals and Alloys, Plenum Press, New York, 1970. https://doi.org/10.1007/978-1-4684-1860-6.
[29] N.J. Petch, The cleavage strength of polycrystals, J Iron Steel InstInst. 174 (1953) 25–28.
[30] Z.C. Cordero, B.E. Knight, C.A. Schuh, Six decades of the Hall–Petch effect – a survey of grain-size strengthening studies on pure metals, Int. Mater. Rev. 61 (2016) 495–512. https://doi.org/10.1080/09506608.2016.1191808.
[31] R.W. Armstrong, 60 years of hall-petch: Past to present nano-scale connections, Mater. Trans. 55 (2014) 2–12. https://doi.org/10.2320/matertrans.MA201302.
[32] S.N. Naik, S.M. Walley, The Hall–Petch and inverse Hall–Petch relations and the hardness of nanocrystalline metals, J. Mater. Sci. 55 (2020) 2661–2681. https://doi.org/10.1007/s10853-019-04160-w.
[33] R. Zheng, J.P. Du, S. Gao, H. Somekawa, S. Ogata, N. Tsuji, Transition of dominant deformation mode in bulk polycrystalline pure Mg by ultra-grain refinement down to sub-micrometer, Acta Mater. 198 (2020) 35–46. https://doi.org/10.1016/j.actamat.2020.07.055.
[34] J. Li, W. Xu, X. Wu, H. Ding, K. Xia, Effects of grain size on compressive behaviour in ultrafine grained pure Mg processed by equal channel angular pressing

at room temperature, Mater. Sci. Eng. A. 528 (2011) 5993–5998. https://doi.org/10.1016/J.MSEA.2011.04.045.
[35] K. Wei, R. Hu, D. Yin, L. Xiao, S. Pang, Y. Cao, H. Zhou, Y. Zhao, Y. Zhu, Grain size effect on tensile properties and slip systems of pure magnesium, Acta Mater. 206 (2021) 116604. https://doi.org/10.1016/j.actamat.2020.116604.
[36] A.P. Zhilyaev, T.G. Langdon, Using high-pressure torsion for metal processing: Fundamentals and applications, Prog. Mater. Sci. 53 (2008) 893–979. https://doi.org/10.1016/j.pmatsci.2008.03.002.
[37] K. Edalati, A. Yamamoto, Z. Horita, T. Ishihara, High-pressure torsion of pure magnesium: Evolution of mechanical properties, microstructures and hydrogen storage capacity with equivalent strain, Scr. Mater. 64 (2011) 880–883. https://doi.org/10.1016/j.scriptamat.2011.01.023.
[38] C.L.P. Silva, I.C. Tristão, S. Sabbaghianrad, S.A. Torbati-Sarraf, R.B. Figueiredo, T.G. Langdon, Microstructure and hardness evolution in magnesium processed by HPT, Mater. Res. 20 (2017) 2–7. https://doi.org/10.1590/1980-5373-MR-2017-0223.
[39] Y. Cao, S. Ni, X. Liao, M. Song, Y. Zhu, Structural evolutions of metallic materials processed by severe plastic deformation, Mater. Sci. Eng. R Rep. 133 (2018) 1–59. https://doi.org/10.1016/j.mser.2018.06.001.
[40] P.C. de Oliveira, L.A. Montoro, M.T. Perez-Prado, A. Hohenwarter, R.B. Figueiredo, A. Isaac, Development of segregations in a Mg–Mn–Nd alloy during HPT processing, Mater. Sci. Eng. A. 802 (2021) 140423. https://doi.org/10.1016/j.msea.2020.140423.
[41] J. Čížek, P. Hruška, T. Vlasák, M. Vlček, M. Janeček, P. Minárik, T. Krajňák, M. Šlapáková, M. Dopita, R. Kužel, T. Kmječ, J.G. Kim, H.S. Kim, Microstructure development of ultra fine grained Mg-22 wt%Gd alloy prepared by high pressure torsion, Mater. Sci. Eng. A. 704 (2017) 181–191. https://doi.org/10.1016/j.msea.2017.07.100.
[42] H. Okamoto, Mg-Nd, J. Phase Equilibria Diffus. 28 (2007) 405. https://doi.org/10.1007/s11669-007-9117-7.
[43] H. Okamoto, Mg-Y (magnesium-yttrium), J. Phase Equilibria Diffus. 31 (2010) 199. https://doi.org/10.1007/s11669-010-9661-4.
[44] H. Okamoto, M.E. Schlesinger, E.M. Mueller, eds., Gd (Gadolinium) Binary Alloy Phase Diagrams, Alloy Phase Diagr. 3 (2016) 0. https://doi.org/10.31399/asm.hb.v03.a0006164.
[45] X.G. Qiao, Y.W. Zhao, W.M. Gan, Y. Chen, M.Y. Zheng, K. Wu, N. Gao, M.J. Starink, Hardening mechanism of commercially pure Mg processed by high pressure torsion at room temperature, Mater. Sci. Eng. A. 619 (2014) 95–106. https://doi.org/10.1016/J.MSEA.2014.09.068.
[46] K. Edalati, Z. Horita, High-pressure torsion of pure metals: Influence of atomic bond parameters and stacking fault energy on grain size and correlation with hardness, Acta Mater. 59 (2011) 6831–6836. https://doi.org/10.1016/j.actamat.2011.07.046.

[47] X.G. Qiao, Y.W. Zhao, W.M. Gan, Y. Chen, M.Y. Zheng, K. Wu, N. Gao, M.J. Starink, Hardening mechanism of commercially pure Mg processed by high pressure torsion at room temperature, Mater. Sci. Eng. A. 619 (2014) 95–106. https://doi.org/10.1016/j.msea.2014.09.068.
[48] S. Tighiouaret, R. Lachhab, A. Hanna, H. Azzeddine, Y. Huang, T. Baudin, A.L. Helbert, F. Brisset, D. Bradai, T.G. Langdon, Thermal Stability of an Mg–Nd Alloy Processed by High-Pressure Torsion, Adv. Eng. Mater. 21 (2019). https://doi.org/10.1002/adem.201900801.
[49] Y.I. Bourezg, H. Azzeddine, T. Baudin, A.L. Helbert, Y. Huang, D. Bradai, T.G. Langdon, Texture and microhardness of Mg-Rare Earth (Nd and Ce) alloys processed by high-pressure torsion, Mater. Sci. Eng. A. 724 (2018) 477–485. https://doi.org/10.1016/j.msea.2018.03.114.
[50] J. Cizek, I. Prochazka, B. Smola, I. Stulikova, V. Ocenasek, R.K. Islamgaliev, O. Kulyasova, The enhanced kinetics of precipitation effects in ultra fine grained Mg alloys prepared by high pressure torsion, Defect Diffus. Forum. 273–276 (2008) 75–80. https://doi.org/10.4028/www.scientific.net/ddf.273-276.75.
[51] O.B. Kulyasova, R.K. Islamgaliev, A.R. Kil'mametov, R.Z. Valiev, Superplastic behavior of magnesium-based Mg-10 wt % Gd alloy after severe plastic deformation by torsion, Phys. Met. Metallogr. 101 (2006) 585–590. https://doi.org/10.1134/S0031918X0606010X.
[52] C.H. Cáceres, D.M. Rovera, Solid solution strengthening in concentrated Mg-Al alloys, J. Light Met. 1 (2001) 151–156. https://doi.org/10.1016/S1471-5317(01)00008-6.
[53] A. Akhtar, E. Teghtsoonian, Solid solution strengthening of magnesium single crystals—I alloying behaviour in basal slip, Acta Metall. 17 (1969) 1339–1349. https://doi.org/10.1016/0001-6160(69)90151-5.
[54] Y.C. Lee, A.K. Dahle, D.H. Stjohn, The role of solute in grain refinement of magnesium, Metall. Mater. Trans. Phys. Metall. Mater. Sci. 31 (2000) 2895–2906. https://doi.org/10.1007/BF02830349.
[55] K. Edalati, D. Akama, A. Nishio, S. Lee, Y. Yonenaga, J.M. Cubero-Sesin, Z. Horita, Influence of dislocation-solute atom interactions and stacking fault energy on grain size of single-phase alloys after severe plastic deformation using high-pressure torsion, Acta Mater. 69 (2014) 68–77. https://doi.org/10.1016/j.actamat.2014.01.036.
[56] C.H. Cáceres, A. Blake, The Strength of Concentrated Mg-Zn Solid Solutions, Phys. Status Solidi A. 194 (2002) 147–158. https://doi.org/10.1002/1521-396X(200211)194:1<147::AID-PSSA147>3.0.CO;2-L.
[57] B.-C. Zhou, S.-L. Shang, Y. Wang, Z.-K. Liu, Diffusion coefficients of alloying elements in dilute Mg alloys: A comprehensive first-principles study, Acta Mater. 103 (2016) 573–586. https://doi.org/10.1016/j.actamat.2015.10.010.
[58] X. Sauvage, A. Duchaussoy, G. Zaher, Strain induced segregations in severely deformed materials, Mater. Trans. 60 (2019) 1151–1158. https://doi.org/10.2320/matertrans.MF201919.

[59] X. Sauvage, Y. Nasedkina, The Role of Grain Boundaries and other Defects on Phase Transformations Induced by Severe Plastic Deformation, Diffus. Found. 5 (2015) 77–92. https://doi.org/10.4028/www.scientific.net/df.5.77.
[60] X. Sauvage, A. Ganeev, Y. Ivanisenko, N. Enikeev, M. Murashkin, R. Valiev, Grain boundary segregation in UFG alloys processed by severe plastic deformation, Adv. Eng. Mater. 14 (2012) 968–974. https://doi.org/10.1002/adem.201200060.
[61] H. Yu, Y. Xin, M. Wang, Q. Liu, Hall-Petch relationship in Mg alloys: A review, J. Mater. Sci. Technol. 34 (2018) 248–256. https://doi.org/10.1016/j.jmst.2017.07.022.
[62] H. Somekawa, T. Mukai, Hall-Petch relation for deformation twinning in solid solution magnesium alloys, Mater. Sci. Eng. A. 561 (2013) 378–385. https://doi.org/10.1016/j.msea.2012.10.040.
[63] Z. Zeng, J.F. Nie, S.W. Xu, C.H.J. Davies, N. Birbilis, Super-formable pure magnesium at room temperature, Nat. Commun. 8 (2017) 1–5. https://doi.org/10.1038/s41467-017-01330-9.
[64] R.B. Figueiredo, S. Sabbaghianrad, A. Giwa, J.R. Greer, T.G. Langdon, Evidence for exceptional low temperature ductility in polycrystalline magnesium processed by severe plastic deformation, Acta Mater. 122 (2017) 322–331. https://doi.org/10.1016/j.actamat.2016.09.054.
[65] H.J. Choi, Y. Kim, J.H. Shin, D.H. Bae, Deformation behavior of magnesium in the grain size spectrum from nano- to micrometer, Mater. Sci. Eng. A. 527 (2010) 1565–1570. https://doi.org/10.1016/j.msea.2009.10.035.
[66] J.A. Sharon, Y. Zhang, F. Mompiou, M. Legros, K.J. Hemker, Discerning size effect strengthening in ultrafine-grained Mg thin films, Scr. Mater. 75 (2014) 10–13. https://doi.org/10.1016/j.scriptamat.2013.10.016.
[67] A. Duchaussoy, X. Sauvage, K. Edalati, Z. Horita, G. Renou, A. Deschamps, F. De Geuser, Structure and mechanical behavior of ultrafine-grained aluminum-iron alloy stabilized by nanoscaled intermetallic particles, Acta Mater. 167 (2019) 89–102. https://doi.org/10.1016/J.ACTAMAT.2019.01.027.
[68] E. Hersent, K. Marthinsen, E. Nes, On the effect of atoms in solid solution on grain growth kinetics, Metall. Mater. Trans. Phys. Metall. Mater. Sci. 45 (2014) 4882–4890. https://doi.org/10.1007/s11661-014-2459-y.
[69] M.M. Abramova, N.A. Enikeev, R.Z. Valiev, A. Etienne, B. Radiguet, Y. Ivanisenko, X. Sauvage, Grain boundary segregation induced strengthening of an ultrafine-grained austenitic stainless steel, Mater. Lett. 136 (2014) 349–352. https://doi.org/10.1016/J.MATLET.2014.07.188.
[70] A. Akhtar, E. Teghtsoonian, Solid solution strengthening of magnesium single crystals-ii the effect of solute on the ease of prismatic slip, Acta Metall. 17 (1969) 1351–1356. https://doi.org/10.1016/0001-6160(69)90152-7.
[71] R. Raj, M.F. Ashby, On grain boundary sliding and diffusional creep, Metall. Trans. 2 (1971) 1113–1127. https://doi.org/10.1007/BF02664244.
[72] M.A. Meyersm, E. Ashworth, A model for the effect of grain size on the yield stress of metals, Philos. Mag. Phys. Condens. Matter Struct. Defects Mech. Prop. 46 (1982) 737–759. https://doi.org/10.1080/01418618208236928.

Chapter 5 – Findings & Future Work

The impact of pressure on microstructural evolution in Mg3Y was investigated across multiple length scales from macro to atomic resolution. The microstructural evolution is generally consistent with other ambient temperature SPD processes for Mg RE with large starting grain size; viz. strain localizes in favorably oriented twins that form in the early stages of deformation and which progressively develop into deformation bands through successive slip and/or twinning. The density of these bands appears to be dependent on pressure, possibly because higher pressure causes more outward flow at the compression stage of HPT which creates a higher initial twin density. The microstructure at all pressures investigated progressively refined within these narrow bands, forming secondary twins and/or developing low angle grain boundaries that transform into high angle boundaries with increased strain. The bands expand and multiply, eventually consuming the entire matrix, though a larger number of turns is required as the pressure is reduced.

Atom probe tomography was used to find the location and configuration of solutes in order to understand their role in the microstructural evolution and subsequent material properties. Small clusters of yttrium less than 10nm in diameter were seen to progressively segregate to boundaries (grain and twin) as a function of strain without any thermal treatment, something that has only recently been reported at twin boundaries for MgY and has not been reported at grain boundaries [1]. The segregation developed non-uniformly, with the level of segregation continuing to develop through the whole range of strains investigated, up to $\varepsilon=57$. This segregation pins grain and twin boundaries,

resulting in very fine grain sizes which exhibited progressive strengthening with strain, exhibiting averaged Vickers hardness values of 50.2±5.6, 63.6±5.3, and 82.2±6.3 at strain of ε=5, 15, and 57 respectively.

Analyzing the strength and grain size as functions of rare-earth solute content as compared to reports in the extant literature shows good agreement with the general trends, solute content allows for finer grains and increases yield strength. By carefully reviewing the literature for alloys that have been confirmed to be in solid solution and subsequently processed by HPT, it is found that no Hall-Petch inversion occurs in the case of solid solution strengthened nanocrystalline Mg-RE alloys. This result is due to the segregation of solutes to boundaries *in-operando,* stabilizing the UFG structures produced and inhibiting grain boundary sliding or rotation which is the commonly cited cause of the yield strength inversion associated with grain size reduction in Mg alloys.

These results together suggest the ability to engineer the microstructure of magnesium rare earth alloys for potential structural applications requiring tailored properties in a lightweight metal. Considering the segregation that occurred in this study, where the concentration of solute was kept within the solutionization region of the equilibrium phase diagram, future work may employ much higher strains and probe the intragranular composition to reveal if solute segregation will reach some equilibrium where the dissolution and segregation rates are balanced. Further, ultra high strain conditions could be considered at various pressures to find if pressure is playing a role in the segregation potential, as has been suggested by diffusion modeling of boundaries under hydrostatic pressure [2].

References

[1] X. Wang *et al.*, "Room Temperature Deformation-induced Solute Segregation and its Impact on Twin Boundary Mobility in a Mg-Y Alloy," *Scr. Mater.*, vol. 209, p. 114375, Mar. 2022, doi: 10.1016/j.scriptamat.2021.114375.

[2] H. Meiser, H. Gleiter, and R. W. Mirwald, "The effect of hydrostatic pressure on the energy of grain boundaries — structural transformations," *Scr. Metall.*, vol. 14, no. 1, pp. 95–99, Jan. 1980, doi: 10.1016/0036-9748(80)90133-7.